2005

Secondary sulfate minerals associated with acid drainage in the eastern US: recycling of metals and acidity in surficial environments

J.M. Hammarstrom
U.S. Geological Survey

R.R. Seal II
U.S. Geological Survey

A.L. Meier
U.S. Geological Survey

J.M. Kornfeld
Dartmouth College

ELSEVIER

Chemical Geology 215 (2005) 407–431

CHEMICAL GEOLOGY
INCLUDING
ISOTOPE GEOSCIENCE

www.elsevier.com/locate/chemgeo

Secondary sulfate minerals associated with acid drainage in the eastern US: recycling of metals and acidity in surficial environments

J.M. Hammarstrom[a,*], R.R. Seal II[a], A.L. Meier[b], J.M. Kornfeld[c]

[a]*U.S. Geological Survey, 954 National Center, Reston, Virginia 20192, USA*
[b]*U.S. Geological Survey, 973 Denver Federal Center, Denver, Colorado 80225, USA*
[c]*Dartmouth College, Dartmouth, New Hampshire, USA*

Accepted 1 June 2004

Abstract

Weathering of metal-sulfide minerals produces suites of variably soluble efflorescent sulfate salts at a number of localities in the eastern United States. The salts, which are present on mine wastes, tailings piles, and outcrops, include minerals that incorporate heavy metals in solid solution, primarily the highly soluble members of the melanterite, rozenite, epsomite, halotrichite, and copiapite groups. The minerals were identified by a combination of powder X-ray diffraction (XRD), scanning electron microscopy (SEM), and electron-microprobe. Base-metal salts are rare at these localities, and Cu, Zn, and Co are commonly sequestered as solid solutions within Fe- and Fe–Al sulfate minerals. Salt dissolution affects the surface-water chemistry at abandoned mines that exploited the massive sulfide deposits in the Vermont copper belt, the Mineral district of central Virginia, the Copper Basin (Ducktown) mining district of Tennessee, and where sulfide-bearing metamorphic rocks undisturbed by mining are exposed in Great Smoky Mountains National Park in North Carolina and Tennessee.

Dissolution experiments on composite salt samples from three minesites and two outcrops of metamorphic rock showed that, in all cases, the pH of the leachates rapidly declined from 6.9 to <3.7, and specific conductance increased gradually over 24 h. Leachates analyzed after 24-h dissolution experiments indicated that all of the salts provided ready sources of dissolved Al (>30 mg L^{-1}), Fe (>47 mg L^{-1}), sulfate (>1000 mg L^{-1}), and base metals (>1000 mg L^{-1} for minesites, and 2 mg L^{-1} for other sites). Geochemical modeling of surface waters, mine-waste leachates, and salt leachates using PHREEQC software predicted saturation in the observed ochre minerals, but significant concentration by evaporation would be needed to reach saturation in most of the sulfate salts. Periodic surface-water monitoring at Vermont minesites indicated peak annual metal loads during spring runoff. At the Virginia site, where no winter-long snowpack develops, metal loads were highest during summer months when salts were dissolved periodically by rainstorms following sustained evaporation during dry spells. Despite the relatively humid climate of the eastern United States, where precipitation typically exceeds evaporation, salts form intermittently in open

* Corresponding author. Tel.: +1 703 648 6165; fax: +1 703 648 6252.
E-mail address: jhammars@usgs.gov (J.M. Hammarstrom).

0009-2541/$ - see front matter. Published by Elsevier B.V.
doi:10.1016/j.chemgeo.2004.06.053

areas, persist in protected areas when temperature and relative humidity are appropriate, and contribute to metal loadings and acidity in surface waters upon dissolution, thereby causing short-term perturbations in water quality.
Published by Elsevier B.V.

Keywords: Sulfate minerals; Mineralogy; Acid rock drainage; Eastern USA

1. Introduction

Secondary sulfate minerals play an important role in acid drainage and metal sequestration in surface environments. Efflorescent blooms of hydrated metal salts have long been recognized as products of evaporation of acid-sulfate waters that form from oxidative weathering of Fe-sulfide and other sulfide minerals. Recent emphasis on the environmental significance of sulfate minerals has spawned a renewed interest in these minerals as indicators of water quality and as monitors of water–rock interactions (Alpers et al., 2000). Because of the high solubility of many of the efflorescent sulfate minerals, climate is an important control on mineral formation and mobilization of metals. In wet climates, salts are ephemeral unless they develop in sheltered areas. In arid climates, or during prolonged dry periods in humid climates, thick crusts of salts can form by evaporative processes, where upward migration of water by capillary action is the dominant process (Olyphant et al., 1991; Dold, 1999). Dissolution of accumulated highly soluble sulfate salts during spring snowmelt runoff or rainstorms can have short-term, catastrophic effects on metal loadings and on aquatic ecosystems (Nordstrom, 1977; Dagenhart, 1980; Olyphant et al., 1991; Bayless and Olyphant, 1993; Keith et al., 2001).

More than 100 inactive or abandoned mines and prospects associated with massive sulfide deposits are documented in the eastern US (Fig. 1). Although most are small, some represent significant, historical mining districts that were active until about 1960. Some minesites have recently become the focus of federal, state, or local remediation activities because of the emanation of acid mine drainage. The cycling of metals and acid by the precipitation and dissolution of efflorescent salts is an important process at these sites. Although similar sulfate-mineral assemblages contribute to acid mine drainage at many coal mines in the eastern US, the base-metal concentrations of minerals and associated waters typically are lower than those observed at base-metal mines (Cravotta, 1994; Rose and Cravotta, 1998; Cravotta et al., 1999).

Secondary sulfate minerals associated with acid drainage in the eastern US include efflorescent salts and Fe- and Al-hydroxysulfate minerals (Palache et al., 1951; Dagenhart, 1980; Cravotta, 1994; Flohr et al., 1995; Byerly, 1996; Coskren and Lauf, 1996; Nordstrom and Alpers, 1999; Bigham and Nordstrom, 2000). Weathering of pyrite [FeS_2] and pyrrhotite [$Fe_{1-x}S$] provides the primary source of Fe and acidity that leads to precipitation of sulfate minerals by myriad processes including oxidation, hydrolysis, and evaporation. A variety of simple hydrated salts can form, among which those of divalent cations have the general formula $M^{2+}SO_4 \cdot nH_2O$, where M=Fe^{2+}, Mg, Zn, Ca, and Cu, as well as mixed divalent–trivalent salts. The most common mineral groups that form efflorescent salts by natural weathering in metal-rich environments include: (1) monoclinic sulfates of the melanterite group, having the general formula $M^{2+}SO_4 \cdot 7H_2O$, where M=Co, Cu, Fe, Mn, Zn; (2) orthorhombic sulfates of general formula $M^{2+}SO_4 \cdot 7H_2O$, where M=Mg, Zn, or Ni; (3) monoclinic sulfates of the hexahydrite group, general formula $M^{2+}SO_4 \cdot 6H_2O$, where M=Co, Cu, Fe, Mg, Mn, Ni, Zn; (4) triclinic sulfates of the chalcanthite group, $M^{2+}SO_4 \cdot 5H_2O$, where M=Cu, Fe, Mg, Mn; (5) monoclinic sulfates of the rozenite group, $M^{2+}SO_4 \cdot 4H_2O$, where M=Co, Cd, Fe, Mg, Mn, Ni, Zn; (6) monoclinic sulfates of the halotrichite group, $AB_2(SO_4)_4 \cdot 22H_2O$, where A=$Fe^{2+}$, Mg, Mn^{2+}, Ni, Zn; B=Al, Cr^{3+}, Fe^{3+}; and (7) triclinic sulfates of the copiapite group, which includes mixed-valence minerals of general formula $A^{2+}Fe_4^{3+}(SO_4)_6(OH)_2 \cdot 18$–$20H_2O$, wherein A=Ca, Cu, Fe, Mg, Zn, and trivalent minerals in the group have the general formula

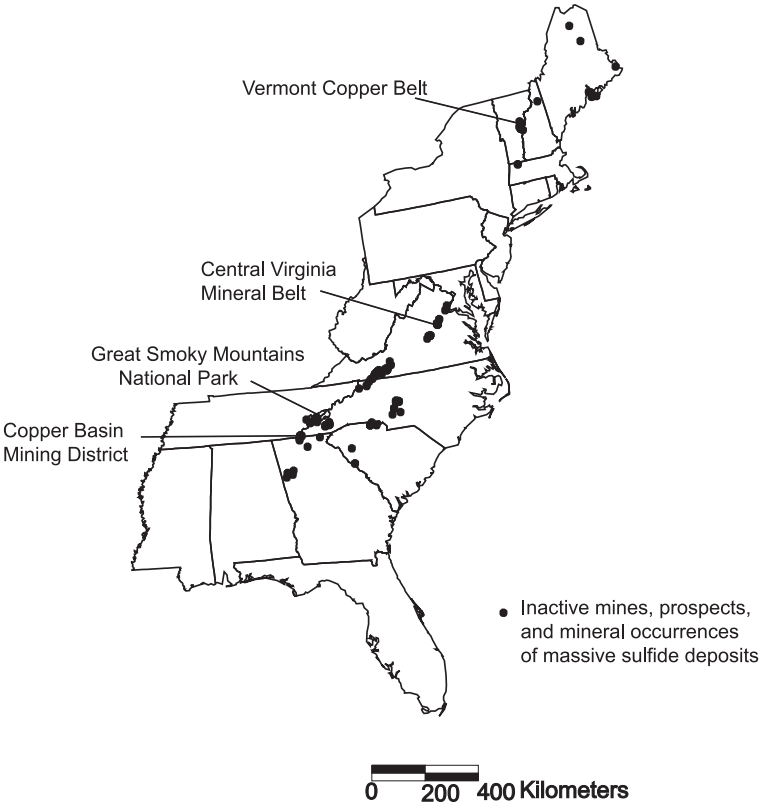

Fig. 1. Study areas. Black dots show locations of inactive mines, prospects, and mineral occurrences classified as massive sulfide-type mineral deposits in the eastern US (McFaul et al., 2000).

$B_{2/3}^{3+}Fe_4^{3+}(SO_4)_6(OH)_2 \cdot 20H_2O$, wherein B=Al, Fe. Iron hydroxysulfate minerals include the characteristic ochre minerals of acid mine drainage, schwertmannite and jarosite. Secondary Al sulfates typically are amorphous, although crystalline alunogen and felsöbányaite (basaluminite) are locally observed.

Surface accumulations of sulfate minerals form by evaporation and precipitation within ponded surface waters, on wet surfaces, at seeps, in groundwater discharges along fractures and cleavages, at discharges from pipes and culverts, and by upward wicking of pore waters in mine-waste and tailings piles by capillary action. Dissolution of sulfate minerals releases metals that can be carried to streams as ionic species in solution, as surface runoff with potential for adverse effects on aquatic ecosystems, or the metals can be localized in wetted surfaces and in ponded waters that repeatedly evaporate, precipitate minerals, and redissolve them, in processes that effectively recycle metals and acidity in surficial environments.

In this paper, we describe field occurrences and mineralogical data for sulfate minerals associated with oxidative weathering of sulfide minerals at several localities in the eastern US. We also compare the effects of sulfate-mineral dissolution on stream metal load as a function of climate. Study areas include (1) inactive mines developed in pyrrhotite-rich, Besshi-type massive sulfide deposits in Vermont and Tennessee, (2) inactive mines developed in pyrite-rich, Kuroko-type massive sulfide deposits in Virginia, and (3) outcrops of sulfide-bearing, regionally metamorphosed sedimentary rocks exposed to weathering in the Great Smoky Mountains (Fig. 1). An alphabetical listing of sulfate minerals identified at these localities in this study and in previous work is given in Table 1, together with nominal mineral formulas.

Table 1
Sulfate minerals[a]

Mineral	Nominal chemical formula	Vermont copper mines	Central Virginia mines	Copper Basin, TN	Great Smoky Mountains, NC, TN
Aluminite	$Al_2(SO_4)(OH)_4 \cdot 7H_2O$				3
Alunogen (s)	$Al_2(SO_4)_3 \cdot 17H_2O$	X	X,1		2,3
Amorphous Al sulfate hydrate		X	X		
Anglesite	$PbSO_4$				X
Antlerite (i)	$Cu_3SO_4(OH)_4$		1		
Apjohnite	$(Mn,Mg)Al_2(SO_4)_4 \cdot 22H_2O$				3
Basaluminite	$Al_4(SO_4)(OH)_{10} \cdot 4H_2O$				3
Bianchite (s)	$(Zn,Fe^{2+})(SO_4) \cdot 6H_2O$		X		
Botryogen	$MgFe^{3+}(SO_4)_2(OH) \cdot 7H_2O$				3
Brochantite (i)	$Cu_4(SO_4)(OH)_6$		1		
Chalcanthite (s)	$CuSO_4 \cdot 5H_2O$	X	1	5	
Copiapite (s)	$Fe^{2+}Fe_4^{3+}(SO_4)_6(OH)_2 \cdot 20H_2O$	X	X,1	X	2
Coskrenite-(Ce)	$(Ce,Nd,La)_2(SO_4)_2(C_2O_4) \cdot 8H_2O$			3	
Destinezite	$Fe_2(PO_4)(SO_4)(OH) \cdot 6H_2O$				3,4
Dietrichite (s)	$(Zn,Fe^{2+},Mn)Al_2(SO_4)_4 \cdot 22H_2O$		X		
Epsomite (s)	$MgSO_4 \cdot 7H_2O$		X,1		2,3
Ferricopiapite (s)	$Fe_{2/3}^{3+}Fe_4^{3+}(SO_4)_6(OH)_2 \cdot 20H_2O$		1		
Ferrohexahydrite (s)	$FeSO_4 \cdot 6H_2O$		1		
Fibroferrite	$Fe^{3+}(SO_4)(OH) \cdot 5H_2O$	X	1	X	X
Goslarite (s)	$ZnSO_4 \cdot 7H_2O$			X	
Gunningite (s)	$ZnSO_4 \cdot H_2O$		1		
Gypsum (i)	$CaSO_4 \cdot 2H_2O$	X	X,1	X	X,2,3
Hexahydrite (s)	$MgSO_4 \cdot 6H_2O$			X	3
Halotrichite (s)	$FeAl_2(SO_4)_4 \cdot 22H_2O$				X,2,3
Jarosite (i)	$KFe_3^{3+}(SO_4)_2(OH)_6$	X	X,1	X	X,2,3
Jurbanite	$Al(SO_4)(OH) \cdot 5H_2O$				3
Linarite (i)	$PbCu^{2+}(SO_4)(OH)_2$		1		
Levinsonite-(Y)	$(Y,Nd,Ce)Al(SO_4)_2(C_2O_4) \cdot 12H_2O$				3
Magnesiocopiapite (s)	$MgFe_4^{3+}(SO_4)_6(OH)_2 \cdot 20H_2O$			X	3
Melanterite (s)	$FeSO_4 \cdot 7H_2O$	X	1	X	2,3
Paracoquimbite (s)	$Fe_2^{3+}(SO_4)_3 \cdot 9H_2O$		1		
Pentahydrite (s)	$MgSO_4 \cdot 5H_2O$		1		
Pickeringite (s)	$MgAl_2(SO_4)_4 \cdot 22H_2O$	X	1		3
Rhomboclase	$(H_3O)Fe^{3+}(SO_4)_2 \cdot 3H_2O$		1		
Rozenite (s)	$FeSO_4 \cdot 4H_2O$	X	1	X	X,2,3
Schwertmannite (i)	$Fe_{16}^{3+}O_{16}(OH)_{12}(SO_4)_2$	X	X	X	3
Serpierite (i)	$Ca(Cu,Zn)_4(SO_4)_2(OH)_6 \cdot 3H_2O$		1		
Siderotil (s)	$Fe^{2+}SO_4 \cdot 5H_2O$	X (Cu)			
Slavikite	$NaMg_2Fe_5^{3+}(SO_4)_7(OH)_6 \cdot 33H_2O$				X,2,3
Starkeyite	$MgSO_4 \cdot 4H_2O$				2
Szomolnokite (s)	$Fe^{2+}SO_4 \cdot H_2O$		1		
Tschermigite	$(NH)_4Al(SO_4)_2 \cdot 12H_2O$				3
Zugshunstite-(Ce)	$(Ce,Nd,La)Al(SO_4)_2(C_2O_4) \cdot 12H_2O$				3

[a] Nominal chemical formulas from Mandarino (1999) except jarosite (Jambor, 1999). X—this study; 1—Dagenhart (1980); 2—Flohr et al. (1995); 3—Coskren and Lauf (2000), 4—Peacor et al. (1999); 5—Palache et al. (1951); (s), highly soluble in water; (i), relatively insoluble in water. In addition to jarosite, both ammoniojarosite and probable hydronium jarosite have been reported to occur at Alum Cave.

Whereas precipitation, rather than evaporation, dominates the climate throughout the eastern US, each of the sites has important seasonal variations in climate that affect the formation and dissolution of sulfates. The Vermont sites experience a winter snowpack and spring melt, whereas the Virginia and

Tennessee sites do not. Furthermore, the Great Smoky Mountains receive the highest annual rainfall (>100 cm) of any area in the eastern US.

2. Methods

Salts were sampled using stainless steel spatulas to separate the salts from substrate. Samples were stored in tightly sealed plastic vials or wrapped in plastic wrap and enclosed in sealed plastic bags. Air temperature and relative humidity conditions were measured in the field with a pocket hygrometer. Powder X-ray diffraction (XRD) and qualitative chemical analysis by scanning electron microscopy (SEM) were used in an iterative fashion to identify the minerals present. Neither technique used alone was sufficient for unambiguous mineral identification because (1) many of the salts form fine-grained mixtures; (2) extensive solid solution typifies many of the sulfate-mineral groups present, so few minerals exactly match nominal end-member powder patterns; (3) grinding during sample preparation can promote changes in hydration state or cause clumping, leading to inaccuracies in XRD relative peak intensities; (4) the sulfate minerals typically produce complex XRD patterns with many overlapping peaks; and (5) energy-dispersion spectra (EDS) identify the major and minor elements present, but do not provide information about hydration state or redox state. Small crystal size, sensitivity of sulfate minerals to beam damage, and difficulty in polishing limit reliable electron-probe microanalysis (EPMA) of most samples. Reported mineral compositions are based on atomic percentages calculated on the basis of anhydrous formulas.

Mineral groups were identified using a Scintag X1 automated powder diffractometer equipped with a Peltier detector with Cu$K\alpha$ radiation. Salts were sorted under a binocular microscope, handpicked, and lightly ground in agate. JADE 5.0 software was used with the JCPDS database (ICCD, 2000) to facilitate mineral identification. Crystal habit, size, and qualitative chemical composition were obtained with a JEOL JSM-840 scanning electron microscope equipped with a backscattered-electron (BSE) detector, a secondary electron (SE) detector, and a PGT X-ray energy-dispersion system. A semiquantitative, standardless software package was used to estimate atomic proportions of elements in salts to verify and refine XRD identifications. Precision of these estimates is on the order of 2% to 5% of the element amount present, based on counting statistics. Mineral compositions by EPMA were obtained with a JEOL-JSX8900 instrument at USGS Laboratories in Reston, Virginia. Selected salt samples were mounted in epoxy and were polished without water. The microprobe, equipped with five wavelength-dispersion spectrometers, was operated at 15 kV. Beam current (20 or 40 nA) and beam diameter were varied to minimize sample damage. Microprobe standards included anhydrite for S, chalcopyrite for Cu, and a variety of silicate, carbonate, and oxide mineral standards for other elements.

Leaching experiments of salts and composite samples of mine waste were performed to compare the geochemistry of resulting solutions with measured surface-water compositions. Composite samples of salts (20 g) from five sites were dissolved in 400 mL of deionized water in a capped polypropylene bottle by shaking the sample for 5 min. Leachate was monitored for pH and specific conductance during the 24-h experiment, after which the leachate was filtered and analyzed for cations and anions (Hageman and Briggs, 2000) in USGS Laboratories by inductively coupled plasma mass spectrometry (ICP-MS) using a multielement method developed by Meier et al. (1994).

Stream waters at the Elizabeth mine and at Valzinco were sampled seasonally over the course of a year. Copperas Brook was sampled monthly; flow was monitored at a weir constructed about 1 km downstream from the Elizabeth minesite (Kornfeld, 2001). Knight's Branch, the stream that flows through the Valzinco tailings, was sampled seasonally (Johnson et al., 2000; Seal et al., 2002). Field procedures for water sampling were based on methods described by Ficklin and Mosier (1999). Water samples were filtered in the field (0.45 μm nitrocellulose filters) and divided into splits for cation and anion analysis. Dissolved total iron and ferrous iron concentrations were determined in the field using a Hach DR2000 spectrophotometer. Cations were analyzed at USGS Laboratories in Denver, Colorado, by ICP-MS and inductively coupled plasma atomic emission spectrometry (ICP-AES). Anions were analyzed by ion

chromatography (chloride and sulfate) and by ion-selective electrode (fluoride) at USGS Laboratories in Ocala, Florida. Saturation indices for salt and tailings leachates, tailings seeps, and stream waters were evaluated with the program PHREEQCI (Parkhurst and Appelo, 1999) using the WATEQ4F database (Ball and Nordstrom, 1991).

3. Site descriptions

3.1. Vermont copper belt

The Vermont copper belt of east–central Vermont (White and Eric, 1944; Slack et al., 1993, 2001; Kierstead, 2001) is a series of pyrrhotite-rich, Besshi-type massive sulfide deposits within the Connecticut River watershed. The largest mine was Elizabeth, which was discovered in 1793 and was developed initially for copperas (melanterite) production from pyrrhotite ore by processes similar to those first described by Agricola (1556). Copper was mined at Elizabeth from the 1830s until 1958, and at the Ely and Pike Hill mines until 1918. Copperas production occurred only at the Elizabeth minesite. Vestiges of the copperas process remain despite later mining for Cu. The geology, environmental geochemistry, and mining history of the Elizabeth and Ely mines were summarized by Hammarstrom and Seal (2001).

Extensive piles of mine waste containing cobble- to boulder-size pieces of partly oxidized, pyrrhotite-rich ore are present at all three minesites. In addition, a 120,000 m^2 (30 acres) accumulation of flotation tailings occupies the stream valley that forms the headwaters of Copperas Brook, the stream that drains the Elizabeth minesite. Significantly fewer flotation tailings are present at Ely and Pike Hill. Acid mine drainage affects streams that drain all three mines. Overall, the mine drainage at the Elizabeth and Ely mines is characterized by acidic to near-neutral pH (1.9 to 6.9), high specific conductance (0.2 to 5.7 mS cm^{-1}), and elevated concentrations of dissolved Fe (0.3 to 1000 mg L^{-1}), Al (0.02 to 236 mg L^{-1}), Cu (up to 200 mg L^{-1}), Zn (up to 38 mg L^{-1}), Co (up to 7 mg L^{-1}), and sulfate (92 to 4900 mg L^{-1}) (Seal et al., 2001). The Elizabeth and Ely mines are listed by the U.S. Environmental Protection Agency as Superfund sites because of ecological impacts on receiving streams (Hathaway et al., 2001).

On humid days, efflorescent salts (melanterite–rozenite mixtures) form white coatings on oxidized ore (Hammarstrom et al., 1999; 2001a,b). The white salts do not blanket fully oxidized mine soils, but form preferentially on exposed ore surfaces, especially along fractures (Fig. 2a). The salts dissolve with the slightest rain event. Site visits included every season over a period of 3 years. During the spring thaw of winter snowpack, snow patches persist at elevations above the salt occurrences, so further melting and rain promote downslope salt dissolution and contribute

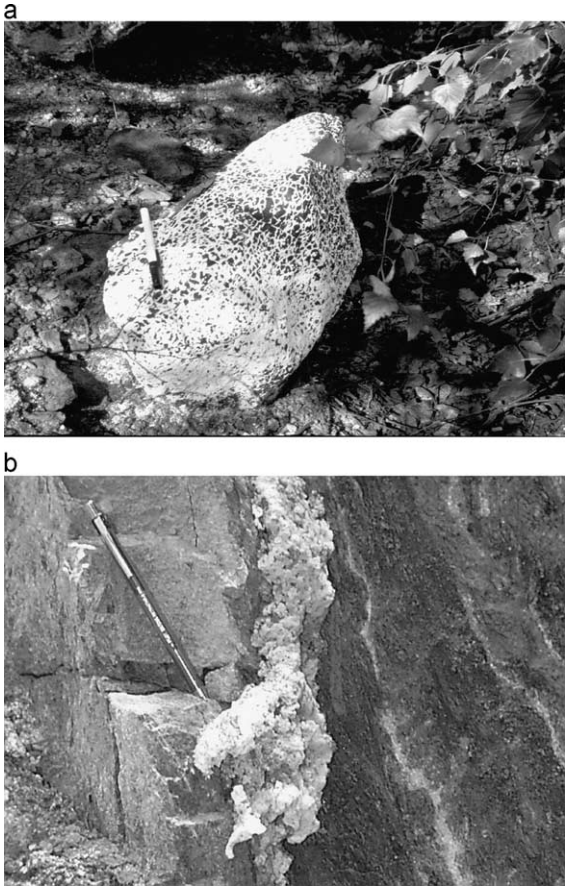

Fig. 2. Field occurrences of efflorescent sulfate salts. (a) "Snowball"-type white salts coat fractures on oxidized pyrrhotite-rich ore on waste dumps at the Ely copper mine, Vermont. (b) Efflorescent salt "bloom" on weathered surface of sulfidic rocks of the Great Smoky Group along the Road-to-Nowhere, at the southeastern corner of Great Smoky Mountains National Park. Note pens for scale in both photos.

acidity and metals to surface runoff on the rising limb of the hydrograph (flushing). In summer, salt crusts form along the rim of the vestigial tailings pond that receives surface runoff from mine wastes upgradient of the tailings. Following rain, globular masses of wet "protosalts" are observed on scrap wood, twigs, and leaf litter, as well as along the walls of erosion gullies. Secondary sulfate salts are also present on outcrops of sulfide-bearing country rocks of the lithologies that host the massive sulfide deposits in the Vermont copper belt. In road cuts several kilometers away from the mined areas, gypsum and pickeringite form centimeter-thick crusts on marble outcrops in partly sheltered areas (Hammarstrom et al., 2001a).

3.2. The Mineral district of central Virginia

The mines of the Mineral district exploited pyrite-rich, Kuroko-type massive sulfide deposits. The Sulphur, Boyd Smith, and Arminius mines were active from about 1835 to 1920 along Contrary Creek, an 8.5-km-long stream that drains into Lake Anna in Louisa County, Virginia. The mines produced pyrite, gossan iron ore, and small amounts of copper. Weathering of pyrite-rich mine waste produces a variety of salts that are localized under protected wall rock overhangs or that form intermittently on mine waste along stream banks. Measurements of stream pH ranged from 3.3 to 6.2 along the length of the creek in July 1998; the lowest pH values were observed immediately downstream of the mine areas. Dagenhart (1980) described 29 secondary sulfate minerals that occurred on Louisa County mine dumps, and demonstrated that salt dissolution during storm runoff increased the peak metal loads in Contrary Creek to as much as 50 times base-flow metal loads. Limited efforts at reclamation in the 1970s had no apparent long-term benefits; the creek is still affected, and the site is currently being considered for further restoration efforts.

The salts persist year-round in a protected area at the Sulphur mine, where a centimeter-thick salt crust coats weathering pyritic schist that forms the host rock for the deposit. Dagenhart (1980) described the occurrence of 24 secondary sulfate minerals at the Sulphur mine; chemical compositions indicated the presence of different varieties of copiapite, all of which incorporated minor amounts of Mn, Zn, and Cu. In addition, magnesian rozenite, melanterite, and zincian pickeringite were reported. Dagenhart observed that melanterite precipitated in periods of high relative humidity early in the day (morning dew), dehydrated to rozenite during the afternoon, and converted back to melanterite later in the day. Rozenite was the dominant ferrous sulfate mineral when we sampled the area. Many of the minerals reported by Dagenhart were observed, but a number of others, including melanterite, szomolnokite, and rhomboclase were not. In samples collected on pyritic schist during dry periods, copiapite was the dominant mineral in the crust, along with alunogen, halotrichite, and jarosite. In contrast to the persistent crust, ephemeral salts form on weathering rock and mine waste in open areas along the banks of Contrary Creek at all three minesites.

In a nearby watershed, oxidation of flotation tailings from Pb–Zn processing at the Valzinco mine produced similar acid mine-drainage conditions (Johnson et al., 2000; Seal et al., 2002). Prior to site reclamation in 2002, a variety of highly soluble white, yellow, and pale blue sulfate minerals coated the tailings on hot, dry days. The salts effloresced on sulfide-rich layers in partly oxidized tailings exposed on the banks of a former process-water pit area below the former flotation mill. Surface runoff from the pit area drained into a stream that flows through tailings (>1500 m^3). Site reclamation completed by the State of Virginia in 2001 included regrading and capping the tailings to shut down the cycle of precipitation and dissolution of sulfate minerals in an effort to improve stream quality.

At both Contrary Creek and Valzinco, streams that flow through mine waste or tailings are acidic (pH<4), elevated in dissolved metals, and are devoid of fish. Fresh pyrite accumulates in deltas that have formed along erosion channels in the tailings lining stream banks. Depending on weather conditions, salts can be observed to form on pyrite accumulated along stream banks. Jarosite precipitates subaqueously in shallow, low-pH pools and seeps along the streams.

3.3. Great Smoky Mountains

Weathering of sulfidic (primarily pyritic) schist, slate, and phyllite of the Anakeesta Formation of the Late Proterozoic Great Smoky Group (King et al.,

1968) produces acid rock drainage severe enough to affect aquatic life (e.g., Huckabee et al., 1975; Kucken et al., 1994). Landslides are common in this lithology (Schultz, 1998), creating temporary, but catastrophic, impacts on aquatic ecosystems. The lithology also poses engineering problems because of the high potential for acid generation associated with exposing fresh pyrite-bearing rock surfaces during construction projects (Tingle, 1995; Byerly, 1996; Schaeffer and Clawson, 1996). Efflorescent sulfate salts coat freshly exposed outcrops in landslide breakaway zones. Iron- and Al-hydroxysulfate minerals precipitate downstream of landslide debris flows (Hammarstrom et al., 2003).

Salts are well-preserved at a popular hiking destination known as Alum Cave Bluff, where more than 20 sulfate minerals, as well as rare-earth oxalate minerals that form in soil below the bluff, are known to occur (Flohr et al., 1995; Coskren and Lauf, 1996, 2000; Lauf, 1997; Peacor et al., 1999). Alum Cave is the type locality for apjohnite, and is one of the few North American localities for slavikite, which forms as masses of yellow-green hexagonal crystals on weathering phyllite. Throughout the region, salts are present where sulfidic rocks of the Great Smoky Group are exposed, such as the Road-to-Nowhere locality at the southeastern corner of the park (Fig. 2b). The Alum Cave and Road-to-Nowhere sites were visited in June of 1997 (wet season) and again in September 1998 (dry season). The abundance of efflorescent salts at Alum Cave varied from visit to visit, although some salts were always present. The specimens that were collected contained copiapite, halotrichite-group minerals, slavikite, and alunogen.

Surface-water quality in the park is affected by acid rain and by oxidative weathering of the sulfidic Anakeesta Formation (Flum and Nodvin, 1995). Streams that drain the Anakeesta Formation are highly variable in pH, ranging from 4.0 to about 7.0. Drip waters and streams immediately below landslides typically have low pH values (~4) and elevated concentrations of dissolved metals relative to other surface waters (Seal et al., 1998).

3.4. Copper Basin, Tennessee

More than a century of copper mining and chemical production in the Copper Basin (Ducktown) mining district in southeastern Tennessee has had a negative impact on aquatic, riparian, and terrestrial ecosystems. Although major reforestation and other restoration efforts have been ongoing since the 1930s, acid mine drainage persists. Moyer et al. (2000) identified a number of factors that contribute to the environmental impacts in the Copper Basin, among which are severe erosion due to devegetation from open-air roasting of massive sulfide ores, oxidation of ores and mine waste, lack of acid-neutralizing potential in the rocks of the region, and accelerated oxidation related to high rates of precipitation and humid conditions. Many of the waste piles have been reclaimed. The Ocoee River watershed, a popular recreational area for water sports and the locus of hydroelectric power dams, has been affected by acid mine drainage, especially along Davis Mill Creek and North Potato Creek. A variety of different types of processed materials is exposed to weathering in open piles along Davis Mill Creek (Moyer et al., 2002; Piatak et al., 2002). Efflorescent salts form on calcine piles, on granulated pellet slag, and on massive cliffs of pot slag; surface runoff from these materials enters Davis Mill Creek. Sulfate minerals were sampled at several localities along Davis Mill Creek and at the abandoned London Mill flotation plant in the North Potato Creek watershed to the west of Davis Mill Creek. The host rocks for the Besshi-type massive sulfide deposits that were mined at Copper Basin are sulfidic members of the Great Smoky Group, the regionally extensive lithology that crops out in Great Smoky Mountains National Park and includes the Anakeesta Formation. For this study, the Copper Basin site was visited only in the spring of 2001. Salts precipitate from ponded acidic water along the streams, at seeps and culvert discharge points, on slag piles, and on abandoned processing-facility structures. Locally, pH values as low as 1.5 were measured in ponded waters. Salts include copiapite, fibroferrite, hexahydrite, melanterite, halotrichite-group minerals, and gypsum.

Water quality is impaired along the entire length of Davis Mill Creek (Moyer et al., 2000). Stream pH ranged from 2.5 to 3.0. Dissolved sulfate locally exceeded 6000 mg L^{-1}, Fe was up to 640 mg L^{-1}, Al to 80 mg L^{-1}, Mn to 210 mg L^{-1}, and Zn to 320 mg L^{-1}.

4. Mineralogy

Pyrite and (or) pyrrhotite are ubiquitous at all of the sites. Generalized possible reaction pathways from primary Fe-sulfide minerals to the secondary sulfate minerals observed in this study are illustrated in Fig. 3. Oxidation by oxygen may not be significant for primary sulfide minerals with molar metal/sulfur ratios=1, such as sphalerite and chalcopyrite; ferric iron is the main oxidant of these minerals in natural systems (Plumlee, 1999). Oxidation of pyrrhotite by O_2 produces an amount of acid commensurate with pyrrhotite composition, typically described by the reaction: $Fe_{1-x}S+(2-x/2)O_2+xH_2O\rightarrow(1-x)Fe^{2+}+SO_4^{2-}+2xH^+$, where 1 mol of pyrrhotite produces a maximum of 0.25 mol of acid. Jambor (2003) proposed an alternative formulation for the pyrrhotite oxidation reaction by writing the reaction for a specific pyrrhotite composition (e.g., Fe_7S_8 in Fig. 3). Thus, the amount of acid produced, 2 mol of H^+ per mol of pyrrhotite, is comparable to the amount of acid produced by pyrite oxidation, in agreement with field observations for pyrrhotite-rich deposits. Oxidation of pyrrhotite of this composition by ferric iron produces

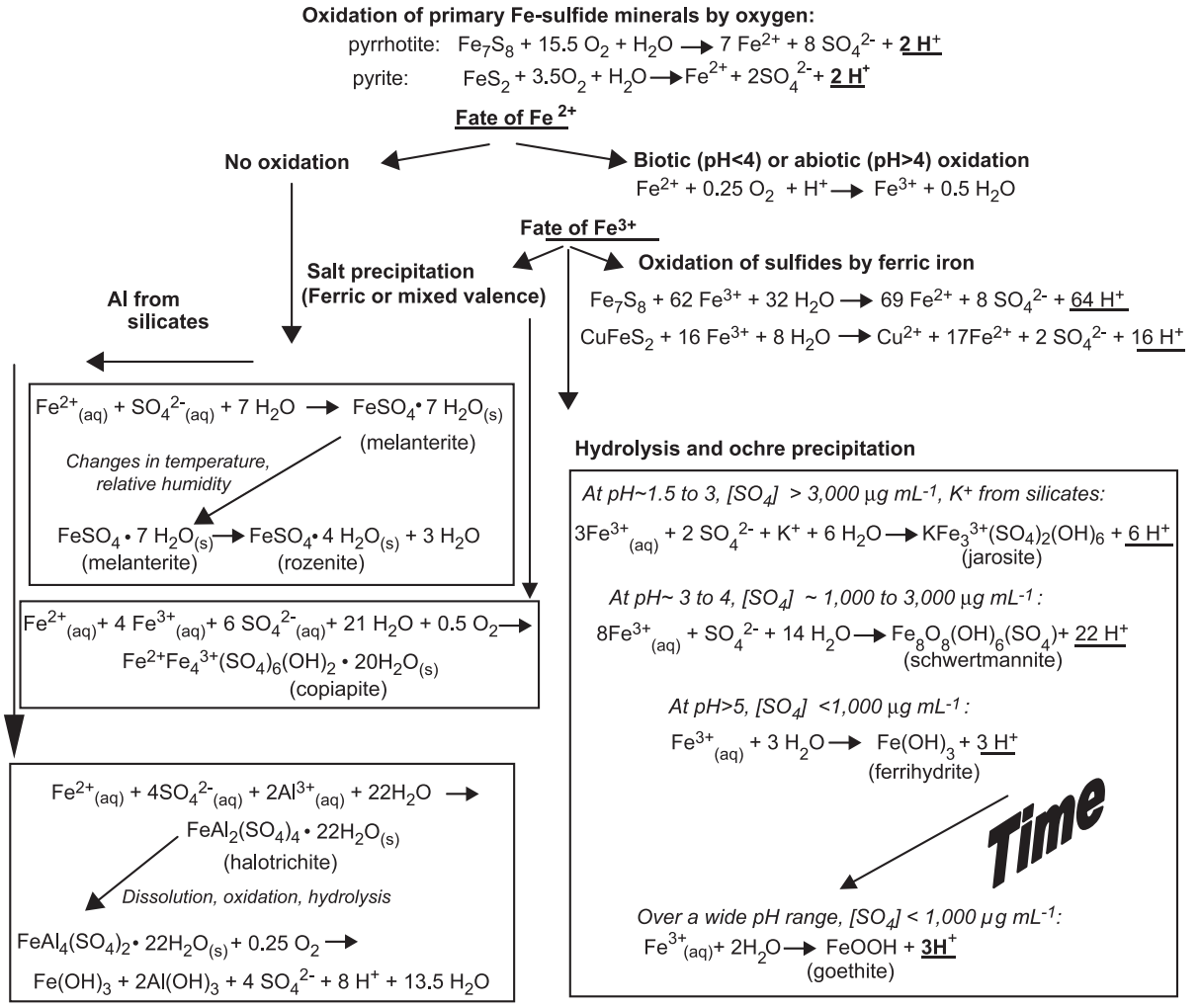

Fig. 3. Processes that lead to secondary sulfate-mineral formation from oxidation of primary Fe-sulfide minerals. Acid-generating steps are underlined. Reactions based on those of Scharer et al. (1994), Bigham (1994), Plumlee (1999), Rose and Cravotta (1998), Bigham and Nordstrom (2000), and Jambor (2003).

64 mol of H^+ per mol of pyrrhotite (Fig. 3), along with ferrous iron and sulfate that may precipitate as early-formed efflorescent sulfate salts (Jambor, 2003; Scharer et al., 1994). A variety of different oxidation pathways may operate in any given setting. Dissolved metals and sulfate can remain in solution or become incorporated in a variety of minerals, depending on the local chemical and physical environment.

4.1. Monoclinic sulfates of the melanterite and rozenite groups

Melanterite [$Fe^{2+}SO_4 \cdot 7H_2O$] is one of the most common soluble sulfate minerals found in nature (Jambor et al., 2000). Melanterite dehydrates to rozenite [$Fe^{2+}SO_4 \cdot 4H_2O$] or to szomolnokite [$Fe^{2+}SO_4 \cdot H_2O$] with increasing temperature and (or) decreasing relative humidity. In the pure system at 20 °C, the melanterite–rozenite transition occurs at 59% relative humidity (Fig. 4; Chou et al., 2002). Solid solution affects the dehydration product. For example, Jambor and Traill (1963) observed that Cu-bearing melanterite dehydrated to siderotil whereas Cu-free melanterite dehydrated to rozenite under the same conditions. Alpers et al. (1994b) proposed a general formula for melanterite-group minerals as $(Fe^{2+}_{1-x-y}Zn_xCu_y)SO_4 \cdot 7H_2O$, where maximum x and y observed in natural samples are 0.307 and 0.654, respectively.

Melanterite sampled for this study typically forms blocky, equant crystals with prominent growth zones (Fig. 5a), or stalactites, and generally includes minor Cu or Zn. White salt crusts on oxidized ore minerals within Vermont mine wastes are composed of rozenite and (or) melanterite, depending on the temperature–humidity conditions. Salts are not apparent early in the morning but develop as the day warms. For example, field measurements of air temperature (T=24.2 °C) and relative humidity (RH=41%) on a June day at noon are consistent with the experimentally determined stability field for rozenite (Fig. 4, Chou et al., 2002) and the XRD confirmation of the presence of rozenite. Samples collected from the same localities under more humid conditions (RH=76%) are also white, but XRD patterns indicated both rozenite and melanterite to be present. Blue salts that formed on a very humid day (RH>90%) were identified as melanterite, with no traces of rozenite. Rosettes of green melanterite and white rozenite grew on a blob of wet, yellow protosalt that, upon drying in the

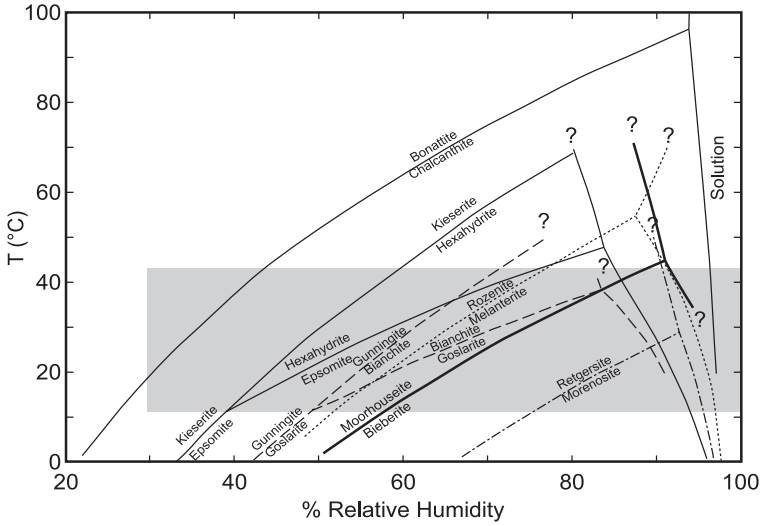

Fig. 4. Hydrogenetic grids for hydrated metal-sulfate salts. Curves represent experimentally determined dehydration reactions in terms of temperature and relative humidity; "?" indicates uncertain reaction phase boundaries. The shaded field represents the general range of temperature and relative humidity conditions in the eastern United States during the summer. Data sources for curves are: (1) melanterite and rozenite (dotted lines); chalcanthite and bonattite (solid line) (Chou et al., 2002), (2) epsomite, hexahydrite, and kieserite (Chou and Seal, 2003a), (3) morenosite and retgersite (dash-dot line) (Chou and Seal, 2003b), (4) bieberite and moorhouseite (heavy line) (Chou and Seal, 2003c), and (5) goslarite, bianchite, and gunningite (dashed lines) (Chou and Seal, this volume).

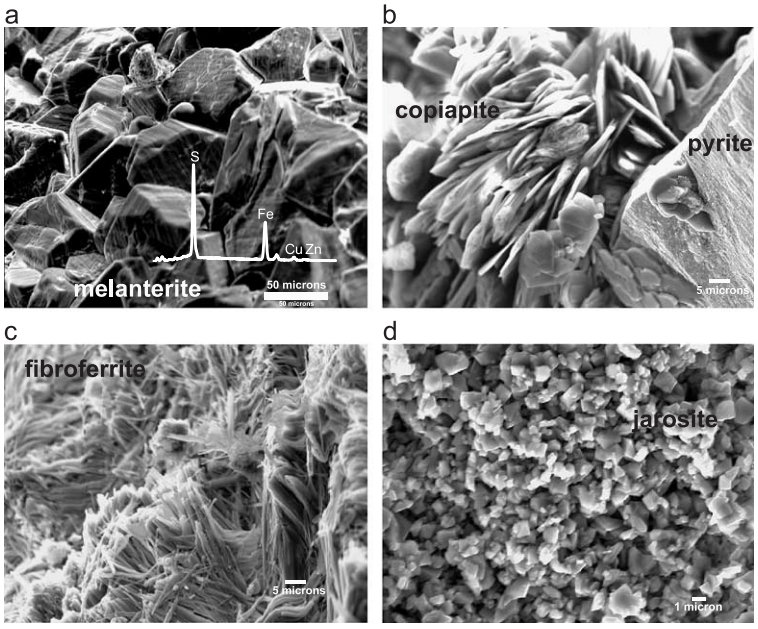

Fig. 5. Secondary-electron images showing varieties of Fe-sulfate salts. (a) Blue Cu-bearing melanterite formed on a weathering calcine pile in Copper Basin; EDS spectrum (0 to 10 keV) shows minor Cu and Zn in the melanterite. (b) Yellow copiapite on pyrite from along Contrary Creek, Virginia. (c) Pinkish brown bundles of fibroferrite on jarosite-rich waste piles at the Elizabeth mine, Vermont. (d) Pseudocubic crystals of jarosite that precipitate as a yellow mud in acidic water (pH=2.6) at the Elizabeth mine, Vermont.

laboratory, crystallized to copiapite. Blue salts that formed on flotation tailings at the Ely mine are melanterite that incorporates solid solution Cu and Co (Hammarstrom et al., 2001b). Accumulations of blue melanterite-group minerals at the Vermont copper mines are a reliable guide to local areas that contain elevated base-metal concentrations in the mine waste and tailings.

Stalactites of green melanterite, up to 4 cm long and 0.5 cm wide, forming on a flotation plant in Copper Basin were sampled. Over the course of a few months, a stalactite stored in mineral oil developed a brownish orange, oxidized coating; part of the same stalactite stored in plastic wrap developed a white powdery rozenite crust. The melanterite displays growth zones on the order of 2 μm wide, but no chemical zoning was detected by X-ray mapping of the zoned area. EPMA analysis (n=7) showed that the melanterite contains 2 wt.% Cu, 0.2 wt.% Zn and has a formula of $(Fe_{0.93}Cu_{0.06}Zn_{0.01})SO_4 \cdot 7H_2O$. Crowley et al. (2003) measured spectral reflectance properties of the melanterite stalactite in the visible to short-wave infrared wavelength range (0.4 to 2.5 μm). In addition to the spectral features for ferrous iron and molecular water, weak crystal-field features suggestive of Fe–O charge transfer, which is compatible with ferric oxide mineral contaminants, were observed. Alpers et al. (1994a) noted that many samples of melanterite contain inclusions of ferric oxide that color the mineral dark green or orange brown. Although no other minerals were identified by XRD shortly after sampling, the stalactite readily oxidized in air and in mineral oil over time.

SEM data confirm that our melanterite-bearing samples that dehydrated to siderotil are Cu-rich relative to those that dehydrate to rozenite. Measurements of relative humidity and air temperature in the field and in ambient laboratory conditions can be compared with metal-sulfate equilibrium curves for pure phases (Fig. 4). XRD and SEM identifications of melanterite sampled on relatively humid days are consistent with the experimental data. Similarly, the absence of melanterite in our samples from Great Smoky Mountains National Park is consistent with the measured relative humidity conditions (RH<20%) at the time. Many of the RH-sensitive salts, such as

melanterite, will dehydrate at ambient laboratory conditions unless preserved in some way (mineral oil, controlled humidity conditions). The humidity-buffer technique of Chou et al. (1998) can be adapted for field use to control the relative humidity environment during sample transport and storage.

4.2. Triclinic sulfates of the chalcanthite group

Salts on Vermont mine-waste soils and flotation tailings include chalcanthite and Cu-bearing siderotil. Pale blue, water-clear crystals on pine needles, on mine waste, and as drusy coatings on damp oxidized tailings-pile surfaces produced an XRD powder pattern that most closely matches siderotil. However, SEM study showed that two minerals are present: (1) pseudohexagonal crystals of siderotil about 10 μm in diameter composed of S, Fe, Cu, and Mg, and (2) unidentified curved bundles of elongate crystals composed of S and Al with subequal amounts of Fe and Cu and minor amounts of Mg (Hammarstrom et al., 1999), which most likely represent a mineral of the halotrichite group. EPMA analysis suggested that the siderotil formula is approximately $(Fe_{0.7}Cu_{0.3})SO_4 \cdot 5H_2O$. On the Ely mine tailings, nearly pure chalcanthite (minor Fe) forms crystals, 100 μm wide, where spring runoff cuts a gully through unoxidized tailings. Field measurements of temperature and relative humidity are consistent with the experimentally determined chalcanthite stability field (Fig. 4).

4.3. Triclinic sulfates of the copiapite group

Copiapite, fibroferrite, jarosite, and schwertmannite are the Fe^{3+}-bearing minerals observed at our sites. Copiapite was less common in exposed settings relative to the melanterite- and halotrichite-group minerals, and apparently forms in environments that are more sheltered. Yellow rosettes of tabular copiapite crystals form on pyritic Anakeesta schist at Alum Cave, and on detrital pyrite sands along Contrary Creek (Fig. 5b). In Vermont, wet blobs of material in erosion gullies and on wood fragments in jarosite-rich mine waste, upon drying in air, crystallized copiapite with or without bundles of pinkish brown fibroferrite crystals (Fig. 5c). EDS spectra for Alum Cave copiapite indicate that Fe and S are the major constituents, with minor Mg and Al.

4.4. Monoclinic sulfates of the halotrichite group

The most common mixed-valence salts encountered in our study are divalent–trivalent solid solutions of halotrichite-group minerals. A variety of different crystal habits has been observed (Fig. 6), but all are elongate rather than equant. The minerals form white, salmon, or yellowish radiating bundles of silky fibers or "hair salts" associated with, or grown upon, simple salts. Halotrichite-group minerals appear to be more stable than melanterite-group minerals at ambient conditions. Jerz and Rimstidt (2003), using a modified version of the humidity-buffer method of Chou et al. (2002), demonstrated an equilibrium humidity of 90% at 25 °C for a natural, halotrichite-rich sample. Fibroferrite- and melanterite-rich samples from the same location, a massive sulfide mine in the Great Gossan Lead of southwestern Virginia, equilibrated at RH 88% and 82%, respectively.

Along Contrary Creek, copiapite formed directly on pyrite surfaces with clusters of pseudohexagonal rozenite crystals, and halotrichite fibers grew on rozenite (Fig. 6a). This same paragenesis is observed at the Vermont sites and has been documented elsewhere (Nordstrom and Alpers, 1999). Aluminum is apparently excluded from the initial minerals that precipitate upon evaporation of the acid-sulfate fluids. During dry summer months, thin crusts of white zincian pickeringite form on tailings along Contrary Creek at the Arminius mine. A variety of Zn-rich white, pink, pale blue, and yellow salts forms intermittently on flotation tailings at the Valzinco mine. The differently colored salts were identified by XRD to be mixtures of minerals of the melanterite, pickeringite, and hexahydrite groups as well as alunogen. SEM and EPMA analyses confirmed the composition of alunogen. However, chemical analysis indicated that compositions of the other minerals do not match the end-member mineral that most closely fit the XRD pattern because Zn is the dominant cation rather than Fe or Mg. EDS data showed that some of the compositions approximate the Zn-rich halotrichite-group mineral, dietrichite, and the Zn-rich equivalent of hexahydrite, bianchite. Fibrous bundles of dietrichite enclose bianchite or goslarite in a texture that resembles cornhusks (Fig. 6c). XRD patterns for Valzinco salts were obtained shortly after the sampling program. Reanalysis of selected samples after a

year showed that the halotrichite-group minerals and alunogen had not changed, but goslarite had dehydrated to a mixture of bianchite and gunningite, and a Zn–Fe hexahydrate mineral had dehydrated to a pentahydrate (i.e., a chalcanthite-group mineral such as siderotil). Chou and Seal (this volume) showed that the goslarite–bianchite transition occurs at a relative humidity of about 60% at room temperature (20 °C); eastern US conditions commonly span this transition (Fig. 4).

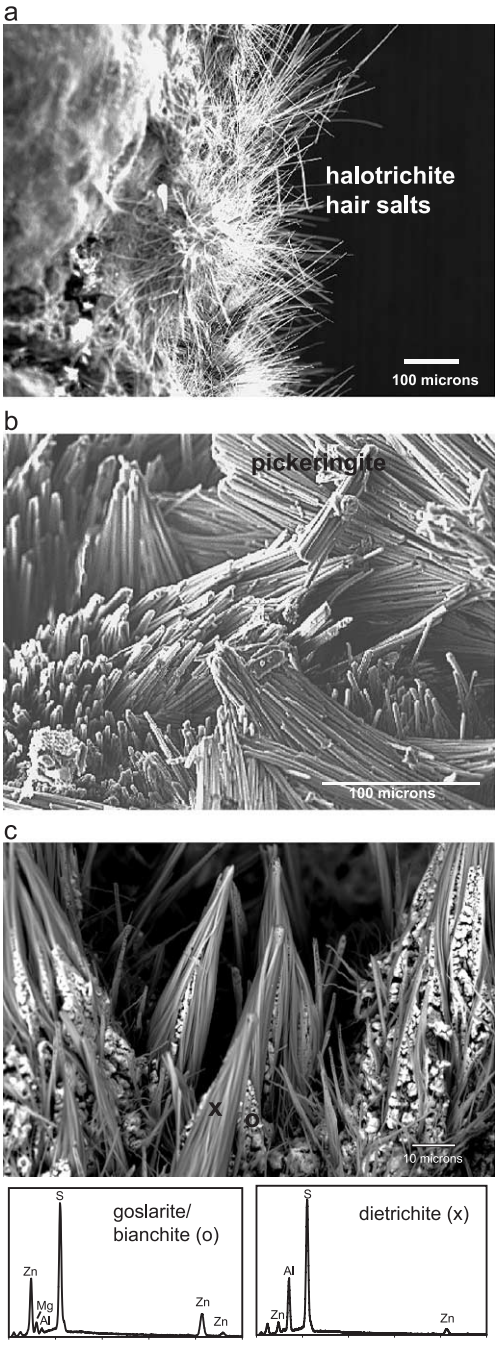

Fig. 6. SEM images of halotrichite-group minerals. (a) Halotrichite hair salts that formed in the laboratory as the outermost phase during drying of a blob of wet, yellow copiapite protosalts on pyrite. (b) Pickeringite from a road cut through pyritic rocks of the Great Smoky Group along the Road-to-Nowhere, North Carolina. (c) Dietrichite laths enclosing goslarite–bianchite on flotation mill tailings at the Valzinco mine, Virginia. EDS spectra (0 to 10 keV) for points "x" and "o" show that the Al-bearing mineral encloses the Al-free mineral. (a) and (b) are secondary-electron images, and (c) is a backscattered-electron image.

Electron microprobe data for the halotrichite-group minerals (Fig. 7a) show that minerals from different localities plot in discrete fields, and data for a given locality exhibit a range of compositions. Compositions of salts from the road cut in Anakeesta Formation along the Road-to-Nowhere plot near end-member pickeringite. Samples from the two Virginia minesites are more Fe-rich, and the Valzinco salts incorporate base metals and approach the composition of dietrichite. The orange color observed for halotrichite-group minerals at Alum Cave is likely due to substitution of Mn, although the possibility of an Fe^{3+} substitution for Al (a bilinite component) cannot be ruled out. In all analyses of our samples, Fe exceeds Mn, thus corresponding to halotrichite rather than apjohnite.

In each of our study areas, the Al-bearing halotrichite-group minerals form late in the paragenetic sequence relative to melanterite–rozenite or copiapite. Experimental data on ternary systems (Fig. 7b, c) provide clues to the observed mineral paragenesis. In the ideal systems, epsomite or melanterite alone coexists with saturated solutions that contain up to about 15 to 20 wt.% $Al_2(SO_4)_3$, respectively (Linke and Seidell, 1958). Tie lines (solid lines) define two 3-phase fields where the halotrichite-group minerals are stable with (1) saturated solutions and alunogen, and (2) saturated solutions and epsomite or melanterite. Saturated solutions that coexist with the halotrichite-group minerals in both systems lie at the H_2O (wt.%) minimum on the solutus. As solutions evaporate (i.e., decrease in wt.% H_2O) at constant temperature, solution composition moves away from the H_2O apex

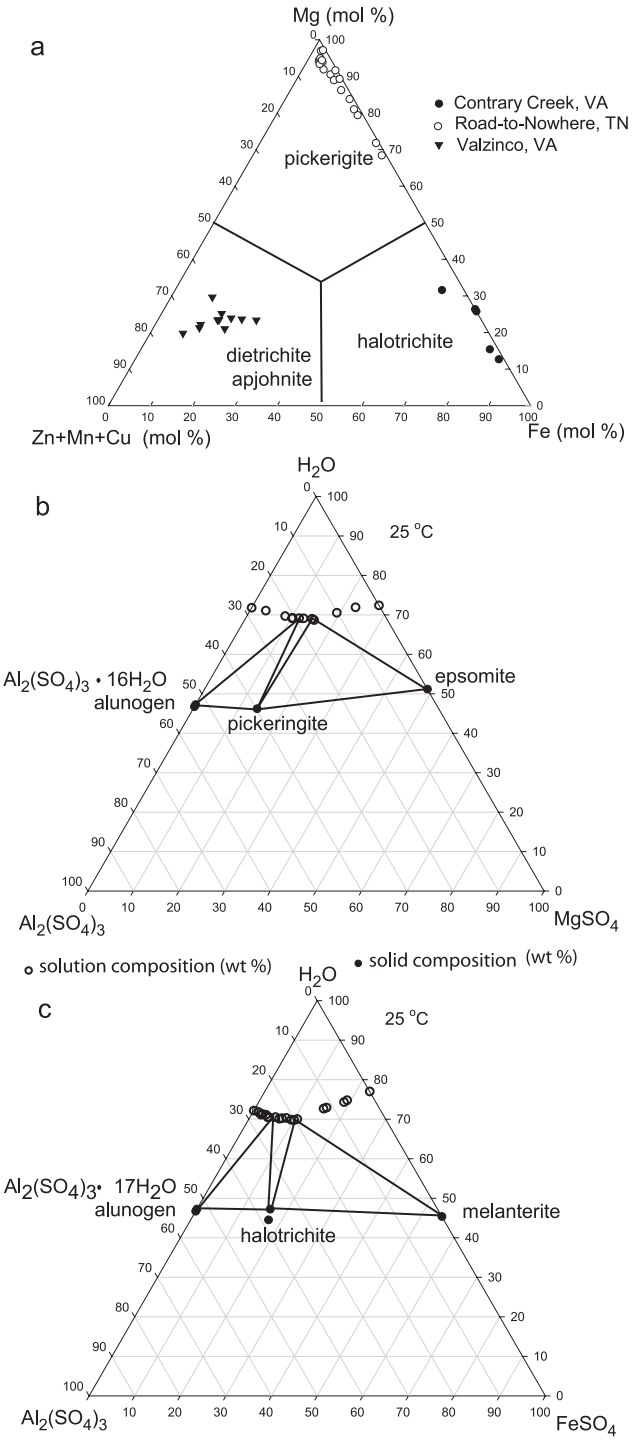
a
Mg (mol %)
Contrary Creek, VA
Road-to-Nowhere, TN
Valzinco, VA
pickerigite
halotrichite
dietrichite
apjohnite
Zn+Mn+Cu (mol %)
Fe (mol %)
b
H2O
25 °C
Al2(SO4)3 • 16H2O
alunogen
epsomite
pickeringite
Al2(SO4)3
MgSO4
solution composition (wt %)
solid composition (wt %)
c
H2O
25 °C
Al2(SO4)3• 17H2O
alunogen
melanterite
halotrichite
Al2(SO4)3
FeSO4

until the saturated-solution composition curve is intersected. Melanterite, for example, should crystallize before the solution composition evolves to halotrichite saturation, for all but the most Al-rich starting solutions; i.e., starting solution with Al/Fe(II) weight ratios greater than about 2 (Fig. 7c). In acid mine drainage, ferrous iron typically exceeds Al in concentration at least until solutions become oxidized.

4.5. Jarosite

Jarosite is a major component of the oxidized mine-waste piles and tailings, especially along the eroded side slopes of tailings piles (Crowley et al., 2001). The jarosite-rich mine-waste soils typically are yellow to yellowish brown and have paste-pH values of less than 2.5. Relatively pure jarosite is precipitating in shallow acidic pools along stream channels at most of our study sites. Associated waters typically have pH<3.1 and ~5000 mg L^{-1} dissolved sulfate. Jarosite forms euhedral, pseudocubic crystals on the order of 1 μm across (Fig. 5d). Microprobe analyses of jarosite from the Elizabeth mine average 6.1±0.6 wt.% K_2O, and 0.45±0.17 wt.% Na_2O, with H_2O of 12.65 wt.% determined by thermogravimetric analysis, thus suggesting an approximate formula of $[K_{0.65}Na_{0.08}(H_3O)_{0.27}]_{\sum 1.00}Fe_3(SO_4)_2(OH)_6$. Multi-element analysis of a bulk sample of jarosite showed that it is not a significant base-metal sink (Hammarstrom et al., 1999).

Jarosite and schwertmannite are precipitating in Davis Mill Creek, where stream pH is typically 2.5 to 3. Jarosite-rich mud forms in puddles and side pools along the edge of the creek. XRD of a bulk sample indicated minor gypsum, quartz, and mica. The jarosite-rich mud contains 33 wt.% Fe, 3.2 wt.% K, and 2500 ppm Cu+Pb+Zn. In contrast, ochre material coating the center of the streambed in an area of higher flow lacked jarosite, consisted of a mixture of schwertmannite and goethite, and contained 40 wt.% Fe, 0.2 wt.% K, and 310 ppm base metals.

4.6. Other sulfate minerals

Gypsum is ubiquitous at most sites under all weather conditions. Although gypsum is slightly soluble in water, it is much less soluble than any of the other sulfate salts found at the study sites. Slavikite was present at Alum Cave in 1997 and 1998, but not on a visit in October 2001. Both slavikite and the associated halotrichite-group minerals appear to be stable under ambient laboratory conditions. No Na was detected in any of the Alum Cave slavikite samples; this observation is consistent with the conclusion of Flohr et al. (1995) that the Alum Cave material fits the stoichiometry $MgFe_3^{+3}(SO_4)_4(OH)_3 \cdot 18H_2O$, as described by Makovický and Streško (1967). The accepted formula for slavikite, $NaMg_2Fe_5^{3+}(SO_4)_7(OH)_6 \cdot 33H_2O$ (Gaines et al., 1997; Mandarino, 1999) is based on the crystal-structure study of Süsse (1973). The crystal structure of Alum Cave material is under study by R. Rouse et al. at the University of Michigan.

The salt compositions reflect the overall chemistry of the mineral deposits or protolith. Mica and chlorite are ubiquitous as gangue and wall rock minerals at all of the study sites. Although mica typically is ranked as intermediate (biotite) to very slow weathering (muscovite), mica, chlorite, and plagioclase are the likely sources of Al. Potassium has not been observed in any of the highly soluble salts, but kalinite $[KAl(SO_4)_2 \cdot 11H_2O]$ is reported to be common at other localities (Keith et al., 1999). Jarosite seems to have been the only secondary mineral to sequester K at our study sites.

5. Geochemistry of mine waters and efflorescent salt leachates

Geochemical modeling typically is performed on natural water samples to evaluate the control of dissolved-metal concentrations by mineral solubility

Fig. 7. Halotrichite-group minerals. (a) Range of EPMA compositions of this study plotted in terms of mole percent. (b) Solution–solid compositions for end-member pickeringite in the system $MgSO_4$–$Al_2(SO_4)_3$–H_2O in terms of weight percent (Bassett and Watt, 1950). (c) Solution–solid compositions for end-member halotrichite in the system $FeSO_4$–$Al_2(SO_4)_3$–H_2O in terms of weight percent (Occleshaw, 1925; Smith, 1942). Experimental data are compiled in Linke and Seidell (1958). The stoichiometry of hydration for the intermediate solids (halotrichite or pickeringite) in some of the original solubility experiments was uncertain, and was later shown to have a 22 H_2O stoichiometry.

(Nordstrom and Alpers, 1999; Alpers and Nordstrom, 1999). We computed saturation indices (SI) for surface waters and leachates from mine-waste soils at selected sites, as well as for salt leachates to compare observed mineral assemblages (Table 1) with SI values predicted by PHREEQC. Saturation indices indicate the thermodynamic tendency of a particular solution to precipitate or dissolve a mineral (Nordstrom and Alpers, 1999; Alpers and Nordstrom, 1999). Negative SI values indicate undersaturation with respect to a given mineral and a tendency for the solution to dissolve that mineral, whereas positive SI values indicate that the mineral is likely to precipitate. Geochemical modeling of aqueous solutions is limited by availability of appropriate thermodynamic data, underlying assumptions of geochemical equilibrium that may or may not apply, availability of complete water-chemistry data for the solution to be modeled, and quality of the data. Jarosite was the only Fe^{3+}-sulfate mineral included in the original WATEQ4 database because thermodynamic data for other minerals were not available. The WATEQ4 database was edited to include data for schwertmannite using the log K_{sp} data reported by Kawano and Tomita (2001) and by Bigham et al. (1996), as well as estimated log K_{sp} values for halotrichite and pickeringite reported by Reardon (1988). The estimated solubility product for schwertmannite of Yu et al. (1999) falls between the values reported by the other two studies. Reardon (1988) estimated log K_{sp} for halotrichite and pickeringite in part from the experimental data for solubility plotted in Fig. 7b and c, as compiled by Linke and Seidell (1958).

Saturation indices were computed for natural drip waters from outcrops of the Anakeesta Formation (samples ACT-1 and RTN-1 from Seal et al., 1998), for surface seeps on mine waste at the Elizabeth mine (LIZM samples from Seal et al., 2001), for an acidic puddle formed by surface runoff from flotation tailings at the Valzinco mine (sample VLZN-10-2), and for composite mine-waste leachates (Table 2). All of the natural waters and leachates have low ionic strength. The Fe^{2+}/Fe^{3+} ratios for leachates were set to match measured oxic surface-water data from Seal et al. (2001). Extreme solution compositions are required for sulfate-mineral precipitation. Frau (2000) showed that hyperacidic saline waters (pH=0.6, 203 g L^{-1} SO_4, Fe^{2+}/Fe_{Total}=0.94) precipitate melanterite at an abandoned pyrite mine in Sardinia, Italy; both PHREEQE (precursor to PHREEQC) and programs incorporating Pitzer equations predicted near-saturation or slight oversaturation in melanterite (SI=−0.9 to 0.15). In our study areas, such extreme unoxidized waters may form locally in direct contact with oxidizing sulfide minerals as soil pore waters or as wetted surfaces. Such solutions are not likely to persist for long without evaporating to produce salts along fractures (such as the rozenite–melanterite rinds on weathering ore shown in Fig. 2), oxidizing to produce ferric iron or mixed-valence minerals, or being diluted. Gypsum, which is ubiquitous at these sites, is always undersaturated in the modeling exercise (SI=−5.65 to −0.67), although SI values approach 0 more closely than those of most of the other sulfate minerals.

For natural waters and mine-waste leachates alike, SI values for schwertmannite, using the data of Bigham et al. (1996), are <0 for all samples. Chemical analyses of two schwertmannite-rich samples (Hammarstrom et al., 1999) from stream-bed ochre deposits at the Elizabeth mine showed that the material is composed mainly of Fe (41 wt.%), S (5.31 wt.%), and O and H. The molar Fe/S ratios for these samples, 4.5, is in good agreement with the molar Fe/S ratio=4.9 reported by Bigham (1994) for the type specimen of schwertmannite and with the molar Fe/S ratio=5.0 for the Bigham et al. (1996) schwertmannite composition used in the PHREEQC simulations. For the Kawano and Tomita (2001) schwertmannite, the molar Fe/S=7.6. This is within the range of chemical compositions reported for natural schwertmannite (molar Fe/S 4.6 to 8.3) summarized by Bigham and Nordstrom (2000). These data illustrate the uncertainties in the nature of schwertmannite and jarosite. The observed ochre minerals may have accumulated and transformed over time. Some of the analyses in Table 2 indicate a SI of >0 for jarosite, but the low concentrations of dissolved sulfate (<500 mg L^{-1}) are contrary to the observations that jarosite generally precipitates from low-pH, sulfate-rich waters (Bigham, 1994; Herbert, 1995). In these cases, the availability of dissolved K drives jarosite saturation. Discrepancies between observed and predicted saturated phases reflect kinetic factors,

Table 2
Chemistry of natural waters and mine-waste leachates associated with efflorescent sulfate salts

	Metal mine oxic surface waters						Mine-waste leachates			
Sample	ACT-1	RTN-1	LIZM11-2	LIZM12-2	LIZM13-2	VLZN-10-2	98JHEly	98JHNPF	TP1-3	VZ-SP1A
Temperature (°C)	14	18	22.6	13.7	24.4	31.1	20	20	20	20
pH	4	4.6	3.74	2.4	2.09	1.1	2.95	3.65	3.58	2.7
Water data in mg L^{-1} (PHREEQCI input data)										
Ca	0.05	0.4	60	59	97	83	14	0.1	170	0.79
Mg	0.45	0.74	12	36	90	900	13	0.14	2.1	11
Na	0.27	0.71	1.7	7.7	9.9	4	0.02	0.22	0.41	0.01
K	0.025	0.43	4.8	0.4	0.28	0.25	0.009	0.33	0.009	0.009
Si	1.4	4.49	7	36	56.1	47	0.19	0.18	0.16	0.009
Fe^{2+}	0.14	0	0.25	0.78	0.18	8930	10.8	0.011	0.048	117
Fe^{3+}	0.18	0.009	0.38	0.92	3.42	4800	25.2	0.025	0.112	63
Al	1.2	0.63	2.2	69	180	800	22	0.018	3.6	16
Cu	0.001	0.0006	0.85	57	110	59	4.6	0.35	0.13	0.43
Zn	0.008	0.021	0.35	11	25	2300	0.45	0.02	0.1	5.4
Pb	0.0002	0	0.0004	0.18	0.00051	2.1	0.00069	0.00077	0.0002	1.5
Ba	0.004	0.004	0.28	0.1	0.1	0.0005	0.0009	0.001	0.0001	0.016
Cl	0.5	0.026	0.5	6.7	6.4	41	0.4	0.5	0.09	1
Mn	0.033	0.6	0.42	49	250	–	0.28	0.0066	0.065	0.53
Cd	–	–	0.0016	0.1	0.22	–	0.0043	0.0001	0.0013	0.013
SO_4	5.9	8	240	1900	4900	53,600	480	15	410	760
Dissolved O_2	9	8	7	11	7	6	–	–	–	–
Phase[a]	*Saturation index*									
Anglesite	−5.50	–	−4.11	−1.17	−3.75	−0.12	−3.75	−4.54	−4.33	−0.37
Barite	−1.71	−1.64	1.14	1.13	0.98	−1.32	−1.20	−2.01	−2.19	0.10
Bianchite	−9.48	−8.91	−6.6	−4.75	−4.37	−2.39	−6.35	−8.66	−7.06	−5.21
Chalcanthite	−9.45	−9.56	−5.31	−3.06	−2.76	−2.98	−4.42	−6.51	−6.02	−5.38
Epsomite	−6.84	−6.51	−4.23	−3.28	−2.94	−1.99	−4.03	−6.98	−4.87	−4.03
Goslarite	−9.19	–	−6.38	−4.46	−4.17	−2.25	−6.12	−8.43	−6.82	−4.97
Gypsum	−5.65	−4.60	−1.32	−0.93	−0.67	−0.83	−1.81	−4.93	−0.77	−2.98
Halotrichite	−23.1	–	−18.2	−14.7	−13.3	−7.48	−14.1	−26.3	−18.19	−13.2
Jarosite(ss)	−3.07	−5.91	0.93	−3.98	−5.68	−2.97	1.59	−5.00	−2.83	1.32
Melanterite	−7.58	−11.08	−6.18	−6.35	−5.90	−1.37	−4.38	−8.34	−6.77	−3.26
Pickeringite	−22.9	−22.8	−16.8	−12.1	−10.9	−8.68	−14.3	−25.5	−16.8	−14.5
Schwertmannite	15.8	8.73	13.9	−8.37	−15.4	−15.1	15.5	4.24	7.85	12.6
Schwertmannite B	−1.93	−9.55	−2.72	−23.15	−29.7	–	−0.15	−12.8	−8.51	−2.65
$Fe(OH)_{3(a)}$	−0.42	−1.17	−0.92	−4.14	−5.13	−5.38	−0.95	−2.01	−1.73	−1.39
Goethite	5.06	4.47	4.89	1.33	0.74	0.73	4.76	3.70	3.98	4.32
Ionic strength	0.0004	0.0004	0.008	0.04	0.08	0.60	0.011	0.0005	0.001	0.002
Charge imbalance	38.6	8.35	−3.56	−34.2	−36.6	5.96	−20.74	−7.48	6.39	−13.4

[a] Phase compositions as listed in Table 1, except as follows: schwertmannite $Fe_8O_8(OH)_{5.9}(SO_4)_{1.05}$ (Kawano and Tomita, 2001); schwertmannite B $Fe_8O_8(OH)_{4.8}(SO_4)_{1.6}$ (Bigham et al., 1996); jarosite(ss) $(K_{0.77}Na_{0.03}H_{0.2})Fe_3(SO_4)_2(OH)_6$; charge imbalance, 100× (cations−|anions|)/(cations+|anions|).

disequilibria processes in natural systems, and uncertainties in redox state and the underlying thermodynamic data.

Calculations indicate that all of the natural waters and mine-waste leachates are saturated in goethite and undersaturated in amorphous ferric hydroxide (Table 2). As noted by Alpers and Nordstrom (1999), goethite is less soluble than ferrihydrite or amorphous $Fe(OH)_3$ and always appears to be supersaturated in low-temperature solutions that are saturated in the other poorly crystalline ochre minerals. All of the ochre minerals are metastable

with respect to goethite over time (Fig. 3); goethite is the most thermodynamically stable Fe-oxide mineral under most soil conditions (Schwertmann and Taylor, 1977). Four years after sampling, the natural waters show no signs of any precipitates. Jarosite was identified by XRD in bottom sediments in the tailings pond where water sample LIZM11-2 was collected; SI values are 0.93 for jarosite solid solution, 0.09 for jarosite sensu stricto, and −3.66 for hydronium jarosite. Jarosite is a major component of Vermont mine-waste samples 98JHNPF and 98JHEly; leachate is undersaturated (SI=−5.00) in the first case, and supersaturated (SI=1.59) in jarosite solid solution in the latter.

Dissolution experiments on bulk samples of salts (20:1 water/solid ratio) from three mine-waste piles and two outcrops of sulfidic metamorphic rock showed that in all cases the pH dropped instantaneously from 6.9 (DI water used in the experiment) to <4 (Table 3). Within another 30 min, pH declined to <3.2 and then decreased slightly over the next 24 h. Chemical analysis of leachates filtered (0.45 μm) after 24 h showed that all of the salts are ready sources of soluble Fe, Al, sulfate, and a variety of other ions (Table 4). No solids precipitated in the leachates. Concentrations of dissolved Al exceeded 30 mg L^{-1} for all samples, reflecting the abundant presence of halotrichite-group minerals and alunogen. Salts sequester significant concentrations of heavy metals (Fig. 8), many of which can pose potential threats to aquatic life. With the exception of the sample from the Valzinco Pb–Zn mine, dissolved concentrations of Pb are one to two orders of magnitude lower than other base-metal concentrations. This reflects the overall Pb-poor character of these settings and the relative insolubility of anglesite (Seal et al., 2000).

Salts associated with outcrops of the Anakeesta Formation (Alum Cave and Road-to-Nowhere samples) contain concentrations of some metals and As (Table 4) that are similar to those in salts from the mine areas. Although rare-earth-element (REE) sulfate–oxalate minerals have been observed only at Alum Cave (Coskren and Lauf, 2000; Rouse et al., 2001), concentrations of REE in the dissolved salt samples from the other localities are similar to, or higher than, the Alum Cave results. Thus, REE are incorporated in efflorescent sulfate salts, are mobile in the environment, and possibly REE minerals may form in acid-drainage settings other than that at Alum Cave.

The highly soluble salts completely dissolved in the leaching experiment. Calculated SI values for most of the observed salts ranged from −1 to −10. The results suggest that the solutions approach saturation in simple metal hydrates such as melanterite or epsomite (SI values of −2 to −4) more closely than they approach saturation in halotrichite-group minerals (SI values of −11 to −13). The ideal end-member mineral compositions in the thermodynamic database used for the speciation calculations are far removed from the observed

Table 3
Geochemical data for leachates of composite efflorescent salt samples from five localities

	Sulphur mine	Arminius mine	Valzinco	Alum Cave outcrop	Road-to-Nowhere outcrop
pH					
0.5 min	2.28	3.40	3.69	2.76	3.36
30 min	2.34	3.13	3.18	2.78	2.93
1 h	2.42	3.03	3.18	2.70	2.92
12 h	2.21	3.00	3.09	2.36	2.86
24 h	2.20	2.98	3.07	2.47	2.84
Specific conductance (mS cm^{-1})					
0.5 min	1.5	3.4	9.2	2.5	3.5
30 min	7.1	7.5	12.0	8.2	12.5
1 h	8.0	7.4	12.0	9.2	12.7
12 h	8.9	7.6	12.0	9.5	12.4
24 h	7.6	7.6	12.0	9.5	12.4

Table 4
Geochemical data for salt leachate at 24 h[a]

	Sulphur mine	Arminius mine	Valzinco mine	Alum Cave outcrop	Road-to-Nowhere outcrop		Sulphur mine	Arminius mine	Valzinco mine	Alum Cave outcrop	Road-to-Nowhere outcrop
Ag	0.03	<0.01	0.1	<0.01	<0.01	Na	0.16	0.22	0.12	0.06	0.21
Al	>30,000	>30,000	>30,000	>30,000	>30,000	Nb	0.2	0.58	0.2	<0.02	<0.02
As	120	<0.2	<0.2	34	7.8	Nd	1400	500	510	1200	200
Au	0.01	0.05	<0.01	<0.01	<0.01	Ni	110	160	970	810	860
Ba	22	11	9.7	17	2	Pb	5.2	7.4	460	0.76	0.2
Be	9.5	33	42	0.7	9.0	Pr	410	120	160	360	56
Bi[1]	0.53	<0.01	0.06	0.02	<0.01	Rb	3.7	1.8	2.7	0.2	6.2
Ca	13	120	36	9.3	7.6	Re	0.06	0.04	0.1	<0.02	0.1
Cd	13	2600	6900	3.2	13	Sb	0.4	0.75	1.0	0.2	<0.02
Ce	3500	880	1400	3400	370	Sc	66	240	89	13	13
Co	660	250	2700	1100	930	Se	<0.2	<0.2	23	<0.2	<0.2
Cr	260	570	260	73	78	SiO_2	<0.5	2	2	<0.5	<0.5
Cs	0.30	0.47	0.05	3.0	7.5	Sm	300	150	110	260	48
Cu	4400	88,000	59,000	900	1200	Sn	1	0.1	<0.05	<0.05	<0.05
Dy	110	120	43	74	25	SO_4	5000	5100	7200	1000	1200
Er	42	58	20	22	7.3	Sr	8.1	82	11	4.6	0.3
Eu	65	79	20	44	15	Ta	0.2	<0.02	0.1	<0.02	<0.02
Fe	>200,000	51,000	>200,000	190,000	71,000	Tb	24	20	9.7	19	5.3
Ga	21	<0.02	<0.02	<0.02	0.3	Th	860	160	260	230	40
Gd	200	130	81	180	37	Ti	290	420	760	58	130
Hf	0.76	<0.05	<0.05	<0.05	<0.05	Tl	<0.05	0.2	<0.05	<0.05	<0.05
Ho	17	22	6.7	9.3	3.2	Tm	5.5	8.8	2.7	2.4	0.81
In	1.3	24	15	0.50	0.1	U	160	450	360	100	57
K	340	160	180	<0.3	<0.3	V	22	2	330	11	5.6
La	850	330	520	1300	68	W	0.3	<0.02	1.6	0.3	0.4
Li	110	250	270	430	790	Y	350	490	180	180	64
Mg	250	460	600	100	120	Yb	37	52	20	14	5.1
Mn	23,000	35,000	77,000	26,000	6100	Zn	1300	610,000	>1,000,000	1200	650
Mo	0.86	0.08	0.73	0.4	0.51	Zr	92	2.6	3.1	3.7	0.3

[a] All values in μg L^{-1} except Ca, Mg, SiO_2, Na, and SO_4, which are mg L^{-1}.

solid–solution compositions. A barite SI of 0.4 for the salt leachate from the Sulphur mine is consistent with SEM observations of barite in salt samples from this site. All minerals were undersaturated in the geochemical modeling of salt leachates, except for barite, goethite, and forms of jarosite, depending on redox assumptions.

6. Effects on water quality

Copperas Brook, which receives most of the surface runoff from the Elizabeth minesite, was sampled at a site 1 km downstream from the mine, monthly in 1999–2000 (Kornfeld, 2001) and weekly during the 2001 period of spring snowmelt. Knight's Branch was sampled downstream from the Valzinco mine seasonally from 1999 to 2001 (Seal et al., 2002). Elevated Cu loads at the Vermont site relative to those at the Virginia site reflect differences in the types of mineral deposits exploited at the two mines (Seal et al., 2001). Peak metal loads at the Elizabeth mine occurred during spring runoff as the winter snowpack melted (Fig. 9). In contrast, metal loads at the Valzinco mine in Virginia were highest during the summer months in response to evaporative concentration during periods of drought punctuated by dissolution events associated with thunderstorms.

In addition to their major-metal contents, soluble salts can temporarily sequester and subsequently release trace metals of potential environmental concern. Cadmium, for example, typically occurs as a

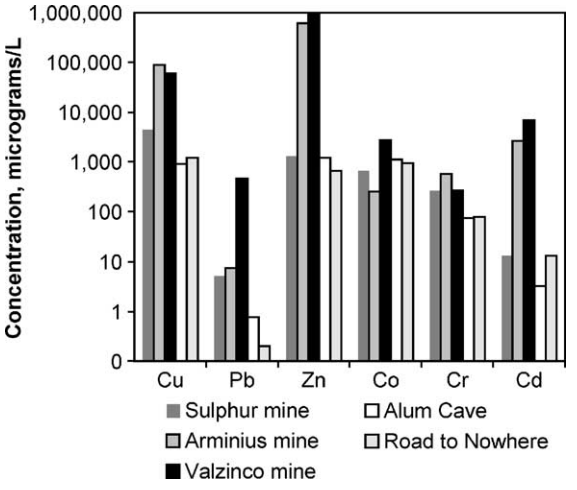

Fig. 8. Metal abundances in efflorescent salt leachates. Salts form on base-metal mine waste at the Sulphur, Arminius, and Valzinco mines. Salts form on pyritic shale away from known mineral deposits at Alum Cave and along the Road-to-Nowhere.

minor element in sphalerite. Weathering of sphalerite leads to precipitation of Zn salts such as goslarite or bianchite, or to incorporation of Zn in solid solutions of Fe^{2+}-bearing minerals, such as those of the melanterite group. The leachate data (Table 4) indicate that Cd is readily released during dissolution of Zn-rich efflorescent salts. Schuiling (1992) reported the presence of Cd in goslarite-rich salt accumulations in Europe and documented seasonal variation in heavy-metal loads in the Geul River as a function of the relative balance between precipitation and evaporation. Although a Cd rozenite-group mineral [$CdSO_4 \cdot 4H_2O$] has been approved (Grice and Ferraris, 2003), natural occurrences of end-member Cd salts are rare.

Year-to-year climate variations complicate prediction of anticipated metal loads. Fig. 10a shows the monthly average discharge for a multiyear period for the Ompompanoosuc River at a stream-gage site a few kilometers downstream from the Elizabeth mine, where stream flow always peaks during spring melt of the winter snowpack. The stream that drains the Valzinco mine is not monitored. Monthly stream-flow data for a monitored stream in Spotsylvania County, near the Valzinco mine, are plotted in Fig. 10b. The Po River watershed is similar in size to the Ompompanoosuc River watershed. Flow in the Po River varies dramatically and can peak in any season. Impacts of salt dissolution are most likely to be high in summer because of the accumulation of salts during dry spells and dissolution during rainstorms. Late-afternoon thunderstorms are common in the summer in this area.

A number of previous studies, many in different climatic settings, have demonstrated the effects that dissolution of metal-sulfate salts during rainfall events has on surface and groundwater (Dagenhart, 1980; Schuiling, 1992; Bayless and Olyphant, 1993; Jambor et al., 2000; Keith et al., 2001). In particular, Dagenhart's (1980) study of Contrary Creek (Sulphur and Arminius mines) showed that spiked increases in dissolved-metal and sulfate concentrations, which occurred during the rising limb of the

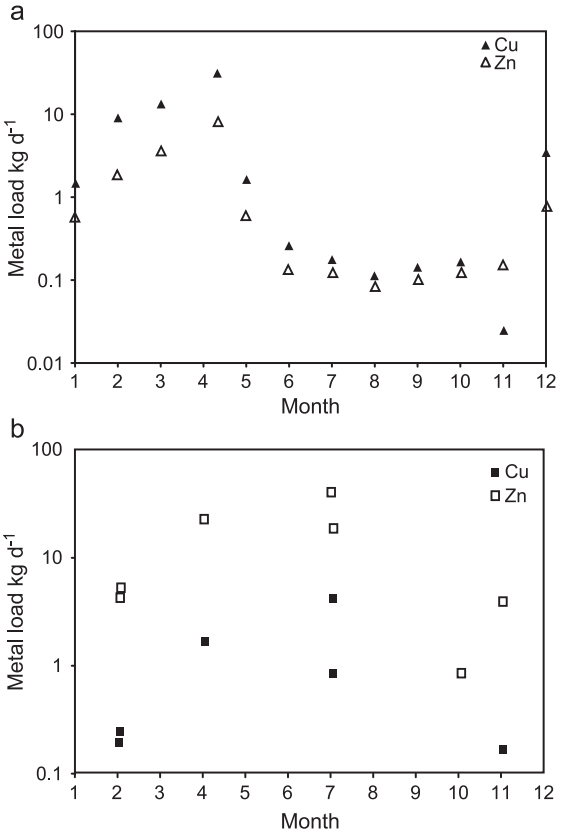

Fig. 9. Seasonal variations in metal loads in streams. (a) Copperas Brook sampled 1 km downstream from the Elizabeth mine, Virginia (Kornfeld, 2001). (b) Knight's Branch sampled 1 km downstream from the Valzinco mine, Virginia (Seal et al., 2002).

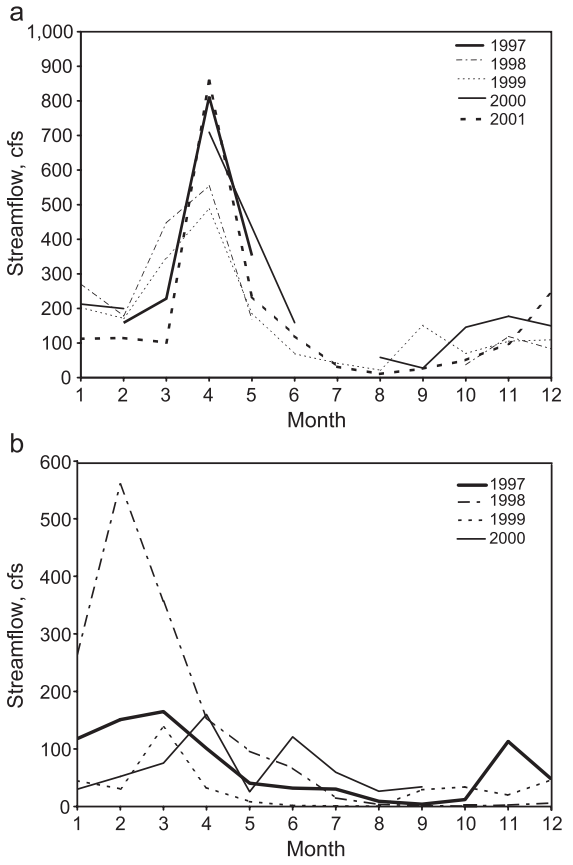

Fig. 10. Yearly variation in monthly average discharge for streams in Vermont and Virginia. Data from USGS National Water Information System (NWIS) for (a) the Ompompanoosuc River at Union Village, Vermont (station 01141500) and (b) the Po River near Spotsylvania, Virginia (station 01673800).

hydrograph following a storm in June 1978, were related to the dissolution of efflorescent salts on mine tailings lining the creek. Our data corroborate this effect at the nearby Valzinco mine and show that spring snowmelts in parts of the eastern US can produce similar effects. In humid climates, dissolution of soluble salts that accumulate during dry periods can have acute or chronic effects on aquatic ecosystems.

7. Conclusions

(1) Sulfidic mine wastes, as well as sulfidic outcrops away from mineral deposits, develop a wide variety of highly soluble efflorescent sulfate salts at a number of locations in the eastern US, including areas where high rainfall occurs.

(2) Sulfate salts can pose determinative challenges because of the complex chemistry of the salts, the common presence of intergrowths of multiple minerals, and instability with respect to temperature and relative humidity.

(3) Metal-sulfate salts are complex solid solutions that may incorporate minor and trace metals, such as Co and Cd, into minerals composed mainly of Fe, Al, Mg, Cu, Mn, and Zn. Although end-member minerals such as bieberite [$CoSO_4 \cdot 7H_2O$] are known to occur as rare minerals, these elements typically are incorporated in the more common efflorescent salts such as melanterite. Trace elements potentially affect aquatic ecosystems when salts are dissolved by waters of low ionic strength (rain, snowmelt). Sulfate minerals cycle Fe, Al, other metals, and S in surface environments.

(4) Salt leachates indicate the potential chemical composition of surface runoff from salt accumulations. The leachates had low pH values and high contents of dissolved solids, characteristic of acid drainage at the sample sites. Speciation calculations for the leachates indicated that the stoichiometric end-members of many of the observed mineral groups dissolve in the simulated runoff experiment.

(5) Modeling of mine-waste leachates that predicted saturation in goethite, and in most cases in jarosite, are in agreement with the observed mineral assemblages.

(6) Observed mineral paragenetic sequences, relative saturation indices, and available experimental data on (Fe,Mg)–Al–SO_4–H_2O mineral systems indicate that halotrichite-group minerals crystallize late relative to simple hydrous metal-sulfate salts. Once formed, the halotrichite-group minerals seem to be stable over a broader range of temperature and relative humidity conditions than are the simple metal-sulfate salts that lack Al as an essential element.

(7) Repeated site visits during different weather conditions are necessary to document the occurrence of efflorescent sulfate minerals in relatively humid climates. Similarly, long-term monitoring

of water quality is necessary to document the seasonality of peak metal loads and maximum metal concentrations to develop adequate remediation schemes for metal-sulfide minesites in the eastern US.

Acknowledgements

The authors thank Nadine Piatak, Adam Johnson, Ryan Barden, John Wormington, Harvey Belkin, and John Jackson for assistance in the field and laboratory work. Reviews by Chuck Cravotta, Allan Kolker, John Jambor, and Charlie Alpers contributed substantially to this paper. The National Park Service, the U.S. Environmental Protection Agency, the Glatfelter Pulp Wood Company, and the Virginia Department of Mines, Mineral, and Energy provided site access and logistical assistance. Trade names are used for descriptive purposes only and do not imply endorsement by the U.S. government. **[PD]**

References

Agricola, G., 1556 [1950]. De Re Metallica. Dover, New York.

Alpers, C.N., Nordstrom, D.K., 1999. Geochemical modeling of water–rock interactions in mining environments. In: Plumlee, G.S., Logsdon, M.J. (Eds.), The Environmental Geochemistry of Mineral Deposits. Part A: Processes, Techniques, and Health Issues, Rev. Econ. Geol., vol. 6A, pp. 289–323.

Alpers, C.N., Blowes, D.W., Nordstrom, D.K., Jambor, J.L., 1994a. Secondary minerals and acid mine-water chemistry. In: Jambor, J.L., Blowes, D.W. (Eds.), Environmental Geochemistry of Sulfide Mine-Wastes, Mineral Assoc. Can. Short Course, vol. 22, pp. 247–270.

Alpers, C.N., Nordstrom, D.K., Thompson, J.M., 1994b. Seasonal variations of Zn/Cu ratios in acid mine water from Iron Mountain, California. In: Alpers, C.N., Blowes, D.W. (Eds.), Environmental Geochemistry of Sulfide Oxidation, Am. Chem. Soc. Symp. Ser., vol. 550, pp. 324–344.

Alpers, C.N., Jambor, J.L., Nordstrom, D.K. (Eds.), 2000. Sulfate Minerals—Crystallography, Geochemistry, and Environmental Significance, Rev. Mineral. Geochem., vol. 40.

Ball, J.W., Nordstrom, D.K., 1991. WATEQ4F—user's manual with revised thermodynamic database and test cases for calculating speciation of major, trace, and redox elements in natural waters. U.S. Geol. Surv. Open-File Rep. 90–129.

Bassett, H., Watt, W., 1950. Pickeringite and the system $MgSO_4$–$Al_2(SO_4)_3$–H_2O. J. Chem. Soc. (London) Part II, 1408–1414.

Bayless, E.R., Olyphant, G.A., 1993. Acid-generating salts and their relationship to the chemistry of groundwater and storm runoff at an abandoned minesite in southwestern Indiana, U.S.A. J. Contam. Hydrol. 12, 313–328.

Bigham, J.M., 1994. Mineralogy of ochre deposits formed by sulfide oxidation. In: Jambor, J.L., Blowes, D.W. (Eds.), Environmental Geochemistry of Sulfide Mine-Wastes, Mineral. Assoc. Can. Short Course, vol. 22, pp. 103–132.

Bigham, J.M., Nordstrom, D.K., 2000. Iron and aluminum hydroxysulfates from acid sulfate waters. In: Alpers, C.N., Jambor, J.L., Nordstrom, D.K. (Eds.), Sulfate Minerals—Crystallography, Geochemistry, and Environmental Significance, Rev. Mineral. Geochem., vol. 40, pp. 351–403.

Bigham, J.M., Schwertmann, U., Traina, S.J., Winland, R.L., Wolf, M., 1996. Schwertmannite and the chemical modeling of iron in acid sulfate waters. Geochim. Cosmochim. Acta 60, 2111–2121.

Byerly, D.W., 1996. Handling acid-producing material during construction. Environ. Eng. Geosci. II (1), 49–57.

Chou, I.-M., Seal II, R.R., 2003a. Determination of epsomite–hexahydrite equilibria by the humidity buffer technique at 0.1 MPa with implications for phase equilibria in the system $MgSO_4$–H_2O. Astrobiology 3, 619–630.

Chou, I.-M., Seal II, R.R., 2003b. Acquisition and evaluation of thermodynamic data for morenosite–retgersite equilibria at 0.1 MPa. Am. Mineral. 88, 1943–1948.

Chou, I.-M., Seal II, R.R., 2003c. Acquisition and evaluation of thermodynamic data for bieberite–moorhouseite equilibria at 0.1 MPa. Geol. Soc. Am. Abstr. Programs 35 (6), 634.

Chou, I.-M., Seal II, R.R., (this volume). Determination of goslarite–bianchite equilibria by the humidity-buffer technique at 0.1 MPa. Chem. Geol.

Chou, I.-M., Seal II, R.R., Hemingway, B.S., 1998. Humidity buffers and their application to the studies of dehydration reactions of sulfate salts at 0.1 MPa. Trans.-Am. Geophys. Union 79, S364.

Chou, I.-M., Seal II, R.R., Hemingway, B.S., 2002. Determination of melanterite–rozenite and chalcanthite–bonattite equilibria by humidity measurements at 0.1 MPa. Am. Mineral. 87, 108–114.

Coskren, T.D., Lauf, R.J., 1996. Secondary sulfates of Alum Cave Bluff, Great Smoky Mountains, Tennessee. Rocks Miner. 71, 192–193.

Coskren, T.D., Lauf, R.J., 2000. The minerals of Alum Cave Bluff, Great Smoky Mountains, Tennessee. Mineral. Rec. 31, 163–175.

Cravotta III, C.A., 1994. Secondary iron-sulfate minerals as sources of sulfate and acidity. In: Alpers, C.N., Blowes, D.W. (Eds.), Environmental Geochemistry of Sulfide Oxidation, Am. Chem. Soc. Symp. Ser., vol. 550, pp. 345–364.

Cravotta III, C.A., Brady, K.B.C., Rose, A.W., Douds, J.B., 1999. Frequency distribution of the pH of coal-mine drainage in Pennsylvania. In: Morganwalp, D.W., Buxton, H. (Eds.), U.S. Geol. Surv. Water-Resour. Invest. Rep. 99-4018A, 313-324.

Crowley, J.K., Mars, J.C., Hammarstrom, J.M., 2001. Airborne imaging spectrometer and field spectroscopic studies of mine wastes at the Elizabeth mine, Vermont. In: Hammarstrom, J.M.,

Seal II, R.R. (Eds.), Environmental Geochemistry and Mining History of Massive Sulfide Deposits in the Vermont Copper Belt, Soc. Econ. Geol. Field Trip Guidebook Ser., vol.35, II, pp. 249–253.

Crowley, J.K., Williams, D.E., Hammarstrom, J.M., Piatak, N.M., Chou, I.-M., Mars, J.C., 2003. Spectral reflectance properties (0.4–2.5 μm) of secondary Fe-oxide, Fe-hydroxide, and Fe-sulphate-hydrate minerals associated with sulphide-bearing mine wastes. Geochem., Explor. Environ. Anal. 3, 219–228.

Dagenhart, T.V. Jr., 1980. The acid mine drainage of Contrary Creek, Louisa County, Virginia—factors causing variations in stream water chemistry. MS Thesis, Univ. Virginia, Charlottesville.

Dold, B., 1999. Mineralogical and geochemical changes of copper flotation tailings in relation to their original composition and climatic setting—implications for acid mine drainage and element mobility. Terre Environ. 18, 1–230.

Ficklin, W.H., Mosier, E.L., 1999. Field methods for sampling and analysis of environmental samples for unstable and selected stable constituents. In: Plumlee, G.S., Logsdon, M.J. (Eds.), The Environmental Geochemistry of Mineral Deposit, Part A. Processes, Techniques, and Health Issues, Rev. Econ. Geol., vol. 6A, pp. 249–264.

Flohr, M.J.K., Dillenber, R.G., Plumlee, G.S., 1995. Characterization of secondary minerals formed as the result of weathering of the Anakeesta Formation, Great Smoky Mountains National Park, Tennessee. U.S. Geol. Surv. Open-File, 95–477.

Flum, T., Nodvin, S.C., 1995. Factors affecting streamwater chemistries in the Great Smoky Mountains, USA. Water Air Soil Pollut. 85, 1701–1712.

Frau, F., 2000. The formation–dissolution–precipitation cycle of melanterite at the abandoned pyrite mine of Genna Luas in Sardinia, Italy—environmental implications. Mineral. Mag. 64, 995–1006.

Gaines, R.V., Skinner, H.C., Foord, E.E., Mason, B., Rosenzweig, A., 1997. Dana's New Mineralogy, 8th ed. Wiley, New York.

Grice, J.D., Ferraris, G., 2003. New minerals approved in 2002 and nomenclature modifications approved in 1998–2002 by the Commission of New Minerals and Minerals Names, International Mineralogical Association. Can. Mineral. 41, 795–802.

Hageman, P.L., Briggs, P.H., 2000. A simple field leach test for rapid screening and qualitative characterization of mine waste dump material on abandoned mine lands. ICARD 2000, Proceedings from the Fifth International Conference on Acid Rock Drainage. Society for Mining, Metallurgy and Exploration (SME), Littleton, Colorado, vol. II, pp. 1463–1475.

Hammarstrom, J.M., Seal II, R.R. (Eds.), Environmental Geochemistry and Mining History of Massive Sulfide Deposits in the Vermont Copper Belt, Soc. Econ. Geol. Field Trip Guidebook Ser., vol. 35, II, pp. 119–293.

Hammarstrom, J.M., Meier, A.L., Jackson, J.C., Barden, R., Wormington, P.J., Wormington, J.D., Seal II, R.R., 1999. Characterization of mine waste at the Elizabeth copper mine, Orange County, Vermont. U.S. Geol. Surv. Open-File Rep. 99-564.

Hammarstrom, J.M., Seal II, R.R., Slack, J.F., Kierstead, M.A., Hathaway, E.M., 2001a. Field trip days 1 and 2: road log for the Elizabeth and Ely mines and vicinity. In: Hammarstrom, J.M., Seal II, R.R. (Eds.), Environmental Geochemistry and Mining History of Massive Sulfide Deposits in the Vermont Copper Belt, Soc. Econ. Geol. Field Trip Guidebook Ser., vol. 35, II, pp. 119–163.

Hammarstrom, J.M., Seal II, R.R., Ouimette, A.P., Foster, S.A., 2001b. Sources of metals and acidity at the Elizabeth and Ely mines, Vermont: geochemistry and mineralogy of solid mine waste and the role of secondary minerals in metal recycling. In: Hammarstrom, J.M., Seal II, R.R. (Eds.), Environmental Geochemistry and Mining History of Massive Sulfide Deposits in the Vermont Copper Belt, Soc. Econ. Geol. Field Trip Guidebook Ser., vol. 35, II, pp. 213–248.

Hammarstrom, J.M., Seal II, R.R., Meier, A.L., Jackson, J.C., 2003. Weathering of sulfidic shale and copper mine waste: secondary minerals and metal cycling in Great Smoky Mountains National Park, Tennessee, and North Carolina, USA. Environ. Geol. 45, 35–57.

Hathaway, E.M., Lovely, W.P., Acone, S.E., Foster, S.A., 2001. The other side of mining—environmental assessment and the process for developing a cleanup approach for the Elizabeth mine. In: Hammarstrom, J.M., Seal II, R.R. (Eds.), Environmental Geochemistry and Mining History of Massive Sulfide Deposits in the Vermont Copper Belt, Soc. Econ. Geol. Field Trip Guidebook Ser., vol. 35, II, pp. 277–293.

Herbert Jr., R.B., 1995. Precipitation of Fe oxyhydroxides and jarosite from acidic groundwater. GFF 117, 81–85.

Huckabee, J.W., Goodyear, C.P., Jones, R.D., 1975. Acid rock in the Great Smokies: unanticipated impact on aquatic biota of road construction in regions of sulphide mineralization. Trans. Am. Fish. Soc. 104, 677–684.

ICCD, 2000. Powder Diffraction File Release 2000 Data Sets 1–50 plus 70–88. International Centre for Diffraction Data, Newton Square, Pennsylvania. (www.icdd.com).

Jambor, J.L., 1999. Nomenclature of the alunite supergroup. Can. Mineral. 37, 1323–1341.

Jambor, J.L., 2003. Mine-waste mineralogy and mineralogical perspectives of acid–base accounting. In: Jambor, J.L., Blowes, D.W., Ritchie, A.I.M. (Eds.), Environmental Aspects of Mine Wastes, Mineral. Assoc. Can. Short Course, vol. 31, pp. 117–145.

Jambor, J.L., Traill, R.J., 1963. On rozenite and siderotil. Can. Mineral. 7, 751–763.

Jambor, J.L., Nordstrom, D.K., Alpers, C.N., 2000. Metal-sulfate salts from sulfide mineral oxidation. In: Alpers, C.N., Jambor, J.L., Nordstrom, D.K. (Eds.), Sulfate Minerals—Crystallography, Geochemistry, and Environmental Significance, Rev. Mineral. Geochem., vol. 40, pp. 303–350.

Jerz, J.K., Rimstidt, J.D., 2003. Efflorescent iron sulfate minerals: paragenesis, relative stability, and environmental impact. Am. Mineral. 88, 1019–1032.

Johnson, A.N., Hammarstrom, J.M., Seal II, R.R., 2000. Mineralogy and geochemistry of sulfidic mine waste at an abandoned Pb–Zn mine—implications for acid-generating and acid-neutralizing potential. Geol. Soc. Am. Abstr. Programs 32, A-181.

Kawano, M., Tomita, K., 2001. Geochemical modeling of bacterially induced mineralization of schwertmannite and jarosite in sulfuric acid spring water. Am. Mineral. 86, 1156–1165.

Keith, D.C., Runnells, D.D., Esposito, K.J., Chermak, J.A., Hannula, S.R., 1999. Efflorescent sulfate salts—chemistry, mineralogy, and effects on ARD streams. Tailings and Mine Waste '99. Balkema, Rotterdam, pp. 573–579.

Keith, D.C., Runnells, D.D., Esposito, K.J., Chermak, J.A., Levy, D.B., Hannula, S.R., Watts, M., Hall, L., 2001. Geochemical models of the impact of acidic groundwater and evaporative salts on Boulder Creek at Iron Mountain, California. Appl. Geochem. 16, 947–961.

Kierstead, M.A., 2001. History and historical resources of the Vermont copper belt. In: Hammarstrom, J.M., Seal II, R.R. (Eds.), Environmental Geochemistry and Mining History of Massive Sulfide Deposits in the Vermont Copper Belt, Soc. Econ. Geol. Field Trip Guidebook Ser., vol. 35, II, pp. 165–191.

King, P.B., Neuman, R.B., Hadley, J.B., 1968. Geology of the Great Smoky Mountains National Park, Tennessee and North Carolina.. U. S. Geol. Surv. Prof. Pap. 587.

Kornfeld, J.M., 2001. Seasonal variations in metal loading to the Ompompanoosuc River from the Elizabeth copper mine. M.A. Thesis, Dartmouth College, Hanover, New Hampshire.

Kucken, D.J., Davis, J.S., Petranka, J.W., Smith, C.K., 1994. Anakeesta stream acidification and metal contamination: effects on a salamander community. J. Environ. Qual. 23, 1311–1317.

Lauf, R.J., 1997. Secondary sulfate minerals from Alum Cave Bluff: microscopy and microanalysis. Oak Ridge Nat. Lab. Rep. ORNL/TM-13471.

Linke, W.F., Seidell, A., 1958. Solubilities of Inorganic and Organic Compounds, 4th ed. Van Nostrand, Princeton, New Jersey.

Makovický, E., Streško, V., 1967. Slavikite from Medzev near Košice, Czechoslovakia. Tschermaks Mineral. Petrogr. Mitt. 12, 100–107.

Mandarino, J.A., 1999. Fleischer's Glossary of Mineral Species 1999. The Mineralogical Record, Tucson, AZ.

McFaul, E.J., Mason Jr., G.T.B., Ferguson, W.B., Lipin, B.R., 2000. U.S. Geological Survey mineral databases-MRDS and MAS/MILS. U.S. Geol. Surv. (Digital Data Ser. DDS-52, 2 disks).

Meier, A.L., Grimes, D.J., Ficklin, W.H., 1994. Inductively coupled plasma mass spectrometry—a powerful analytical tool for mineral resource and environmental studies. U.S. Geol. Surv. Circ. 1103-A, 67–68.

Moyer, T.C., Jourdan, R., Taylor, M., Mozingo Jr., J.T., 2000. Challenges of restoring an environment impacted by a century of copper mining: the Copper Basin mining district, Tennessee. Geol. Soc. Am. Abstr. Programs 32, A476–A477.

Moyer, T.C., Dube, T.E., Johnsen, M.G., 2002. The impacts of hardrock mining in eastern Tennessee—integrated studies of Davis Mill Creek and the Copper Basin mine site. Geol. Soc. Am. Abstr. Programs 34, 143–144.

Nordstrom, D.K., 1977. Hydrogeochemical and microbiological factors affecting the heavy metal chemistry of an acid mine drainage system. PhD thesis, Stanford Univ., Stanford, California.

Nordstrom, D.K., Alpers, C.N., 1999. Geochemistry of acid mine waters. In: Plumlee, G.S., Logsdon, M.J. (Eds.), The Environmental Geochemistry of Mineral Deposits: Part A. Processes, Techniques, and Health Issues, Rev. Econ. Geol., vol. 6A, pp. 133–160.

Occleshaw, V.J., 1925. The equilibrium in the systems aluminum sulphate–copper sulphate–water and aluminum sulphate–ferrous sulphate–water at 25°. J. Chem. Soc. (London), 2598–2602.

Olyphant, G.A., Bayless, G.R., Harper, D., 1991. Seasonal and weather-related controls on solute concentrations and acid drainage from a pyritic coal-refuse deposit in southwestern Indiana, USA. J. Contam. Hydrol. 7, 219–236.

Palache, C., Berman, H., Frondel, C., 1951. The System of Mineralogy, vol. II, 7th ed. Wiley, New York.

Parkhurst, D.L., Appelo, C.A.J., 1999. User's guide to PHREEQC (Version 2)—a computer program for speciation, batch-reaction, one-dimensional transport, and inverse geochemical calculations. U.S. Geol. Surv. Water-Resour. Invest. Rep. 99-4259 http://wwwbrr.cr.usgs.gov/projects/GWC_coupled/phreeqc/index.html.

Peacor, D.R., Rouse, R.C., Coskren, T.D., Essene, E.J., 1999. Destinezite ("diadochite"), $Fe_2(PO_4)(SO_4)(OH)\cdot 6H_2O$: its crystal structure and role as a soil mineral at Alum Cave Bluff, Tennessee. Clays Clay Miner. 47, 1–11.

Piatak, N.M., Seal II, R.R., Hammarstrom, J.M., 2002. Mineralogical and geochemical controls on the release of trace elements from slag produced by base- and precious-metal smelting at abandoned mine sites. Geol. Soc. Am. Abstr. Programs 34, 296.

Plumlee, G.S., 1999. The environmental geology of mineral deposits. In: Plumlee, G.S, Logsdon, M.J. (Eds.), The Environmental Geochemistry of Mineral Deposits: Part A. Processes, Techniques, and Health Issues, Rev. Econ. Geol., vol. 6A, pp. 71–116.

Reardon, E.J., 1988. Ion interaction parameters for $AlSO_4$ and application to the prediction of metal sulfate solubility in binary salt systems. J. Phys. Chem. 92, 6426–6431.

Rose, A.W., Cravotta III, C.A., 1998. Geochemistry of coal-mine drainage. In: Smith, M.W., Brady, K.B. (Eds.), The Prediction and Prevention of Acid Drainage from Surface Coal Mines in Pennsylvania. Pennsylvania Department of Environmental Protection. (chap. 1).

Rouse, R.C., Peacor, D.R., Coskren, T.D., Essene, E.J., Lauf, R.J., 2001. The new minerals levinsonite-(Y) [$(Y,Nd,Ce)Al(SO_4)_2(C2O4)\cdot 12H_2O$] and zugshunstite-(Ce) [$(Ce,Nd,La)Al(SO_4)_2(C_2O_4)\cdot 12H_2O$]-coexisting oxalates with different structures exhibiting strong differentiation of LREE and HREE. Geochim. Cosmochim. Acta 65, 1101–1115.

Schaeffer, M.F., Clawson, P.A., 1996. Identification and treatment of potential acid-producing rocks and water quality monitoring along a transmission line in the Blue Ridge Province, southwestern North Carolina. Environ. Eng. Geosci. 2, 35–48.

Scharer, J.M., Nicholson, R.V., Halbert, B., Snodgrass, W.J., 1994. A computer program to assess acid generation in pyritic tailings. In: Alpers, C.N., Blowes, D.W. (Eds.), Environmental Geochemistry of Sulfide Oxidation, Am. Chem. Soc. Symp. Ser., vol. 550, pp. 132–152.

Schuiling, R.D., 1992. Goslarite—threat or promise for the environment of the Geul Valley? J. Geochem. Explor. 42, 383–386.

Schultz, A.P., 1998. Geologic map of the Mount LeConte 7.5 minute quadrangle, Great Smoky Mountains National Park, Tennessee and North Carolina. U.S. Geol. Surv. Open-File Rep. 98-32.

Schwertmann, U., Taylor, R.M., 1977. Iron oxides. In: Dixon, J.B., Weed, S.B. (Eds.), Minerals in Soil Environments, Soil Sci. Soc. Am. Book Ser., vol. 1, pp. 145–180.

Seal II, R.R., Hammarstrom, J.M., Southworth, C.S., Meier, A.L., Haffner, D.P., Schultz, A.P., Plumlee, G.S, Flohr, M.J.K., Jackson, J.C., Smith, S.M., Hageman, P.L., 1998. Preliminary report on water quality associated with the abandoned Fontana and Hazel Creek mines, Great Smoky Mountains National Park, North Carolina and Tennessee. U.S. Geol. Surv. Open-File Rep. 98-476.

Seal II, R.R., Hammarstrom, J.M., Foley, N.K., Alpers, C.N., 2000. Geoenvironmental models for seafloor base- and precious-metal massive sulfide deposits—tools for mitigation and remediation. ICARD 2000, Proceedings from the Fifth International Conference on Acid Rock Drainage, Society for Mining, Metallurgy and Exploration (SME), Littleton, Colorado, vol. II, pp. 151–160.

Seal II, R.R., Kornfeld, J.M., Meier, A.L., Hammarstrom, J.M., 2001. Geochemical settings of mine drainage in the Vermont copper belt. In: Hammarstrom, J.M., Seal II, R.R. (Eds.), Environmental Geochemistry and Mining History of Massive Sulfide Deposits in the Vermont Copper Belt, Soc. Econ. Geol. Field Trip Guidebook Ser., vol. 35, II, pp. 255–276.

Seal, R.R., Johnson, A.N., Hammarstrom, J.M., Meier, A.L., 2002. Geochemical characterization of drainage prior to reclamation at the abandoned Valzinco Mine, Spotsylvania County, Virginia. U.S. Geol. Surv. Open-File Rep. 02-360.

Slack, J.F., Offield, T.W., Shanks, W.C., Woodruff III, L.G., 1993. Besshi-type massive sulfide deposits of the Vermont copper belt. Soc. Econ. Geol. Guidebook Ser. 17, 32–73.

Slack, J.F., Offield, T.W., Woodruff, L.G., Shanks II, W.C., 2001. Geology and geochemistry of Besshi-type massive sulfide deposits, Vermont copper belt, U.S.A. In: Hammarstrom, J.M., Seal II, R.R. (Eds.), Environmental Geochemistry and Mining History of Massive Sulfide Deposits in the Vermont Copper Belt, Soc. Econ. Geol. Field Trip Guidebook Ser., vol. 35, II, pp. 193–211.

Smith, N.O., 1942. The hydration of aluminum sulfate. J. Am. Chem. Soc. 64, 41–44.

Süsse, P., 1973. Slavikite: Kristallstruktur und chemische Formel. Neues Jahrb. Mineral., 93–95.

Tingle, A.R., 1995. A geochemical assessment of highway construction through sulfidic rocks. MS thesis, Univ. Tennessee, Knoxville.

White, W.S., Eric, J.H., 1944. Preliminary report on the geology of the Orange County copper district, Vermont. U.S. Geol. Surv. Open-File Rep.

Yu, J.Y., Heo, B., Choi, I.K., Cho, J.P., Chang, H.W., 1999. Apparent solubilities of schwertmannite and ferrihydrite in natural stream waters polluted by mine drainage. Geochim. Cosmochim. Acta 63, 3407–3416.